

# A novel strategy for the treatment of osteoarthritis by restoring joint homeostasis using natural antagonists

Inez Duursma

Developmental BioEngineering  
University of Twente

Examination committee:  
Prof. Dr. H.B.J. Karperien  
Dr. Ing. J.N. Post  
Dr. R. Bansal  
M. Koerselman  
S. Khurana

UNIVERSITY OF TWENTE.

## Preface

This report is written at the Developmental BioEngineering group as a completion of my master thesis for my Master's in Biomedical Engineering at the University of Twente. Several persons have contributed to my academic and practical development during the nine months that I worked on this thesis. I would specifically like to thank my main supervisor Dr. Ing. Janine Post for her feedback, great insights and advice during our three-weekly meetings. I would also like to thank Michelle Koerselman and Sakshi Khurana for their advice during these same meetings. I have experienced those meetings as extremely helpful and educational. In addition, I would like to thank Michelle Koerselman and Sakshi Khurana for their daily supervision in the lab. I will never forget the first time I dissected a bovine knee together with Michelle. I felt like a construction worker and medical doctor at the same time. I would also like to thank Dr. Kannan Govindaraj for his help with the luciferase assays and Carlo Paggi for his help with the quantification of the immunohistochemical results. Furthermore, I would like to thank Prof. Dr. Marcel Karperien for being the chair of my graduation committee and Dr. Ruchi Bansal for being my external member in my graduation and their feedback at the mid-term meeting. I would like to end by thanking all employees and students working at the Developmental BioEngineering group for their help and the great time I had.

## Abstract

Undesirable chondrocyte hypertrophy and terminal differentiation cause matrix degeneration and calcification and are characteristics of osteoarthritis. Maintaining the chondrogenic phenotype and avoiding hypertrophy remain a big challenge in cell-based therapeutic strategies. Targeting signalling pathways holds great potential for the development of therapies for OA. However, we need to gain insight in the regulation of those signalling pathways in the early stages of OA development.

WNT pathway antagonists DKK1 and FRZB have been identified as possible key factors in the onset of osteoarthritis. In this study, we investigated the role of DKK1 and FRZB in the onset of osteoarthritis in bovine osteochondral plugs with specifically designed variable domain of single chain heavy chain only antibodies (VHH). To accomplish this, an experimental set-up has been established and the biological activity and binding characteristics of the VHHs was determined.

It was revealed that isolated bChs can be used as a control cell line, bovine osteochondral plugs can be cultured stably for at least 28 days and Kristensen's is the best decalcification technique. It was also found that in OA typically the cartilage thickness decreases, the cell density increases, the cellular diameter increases and the pericellular matrix of collagen I and II increases. Unfortunately, the VHHs were not able to neutralize DKK1 and FRZB, possibly because the VHH's lost their biological activity due to long-term storage.

To conclude, this research provides a platform to gain insight in the cellular mechanism involved in the onset of osteoarthritis. With the characterization of fresh VHHs, research can be continued. It sets the stage for the development of knowledge which can lead future therapies that are able to halt the development of osteoarthritis.

## Samenvatting

Hypertrofie en terminale differentiatie van chondrocyten veroorzaken matrix degeneratie en verkalking en zijn de belangrijkste kenmerken van osteoarthritis. Het chondrogene fenotype behouden en hypertrofie vermijden blijft een grote uitdaging in therapeutische strategieën gebaseerd op cellen. Onderzoek naar de specifieke signaaltransductie in de cel biedt potentie voor de ontwikkeling van therapieën voor artrose. Om de huidige kenniskloof te overbruggen, moeten we echter inzicht verwerven in de regulering van die signaaltransductie in de vroege fase van het ontstaan van artrose.

WNT signaaltransductie antagonisten DKK1 en FRZB zijn geïdentificeerd als mogelijke sleutelfactoren bij het ontstaan van artrose. In deze studie onderzochten we de rol van DKK1 en FRZB bij het ontstaan van artrose in osteochondraal weefsel van koeien met een specifiek ontworpen variabel domein van enkelvoudige keten antilichamen met alleen zware ketens (VHH). Om dit te bereiken is een experimentele opstelling opgezet voor het osteochondraal weefsel en zijn de biologische activiteit en bindingskenmerken van de VHHs bepaald.

Er werd onthuld dat geïsoleerde koeien-chondrocyten uit de knie kunnen worden gebruikt als een controle cellijn, koeien osteochondraal weefsel stabiel gekweekt kan worden voor minstens 28 dagen en dat 'Kristensens' de beste ontkalkingstechniek is. Er werd ook gevonden dat bij artrose typisch de kraakbeendikte afneemt, de cel dichtheid toeneemt, de cel diameter toeneemt en de pericellulaire matrix van collageen I en II toeneemt. Helaas konden de VHHs DKK1 en FRZB niet neutraliseren door het opslaan van de VHHs voor langere tijd waardoor ze hun biologische activiteit zijn verloren

Tot slot biedt dit onderzoek een platform om inzicht te krijgen in het cellulaire mechanisme dat betrokken is bij het ontstaan van artrose. Met de karakterisering van nieuwe VHHs kan het onderzoek worden voortgezet. Het vormt de basis voor de ontwikkeling van kennis die kan leiden tot toekomstige therapieën voor artrose.

## Table of Contents

Introduction.....	9
Articular Cartilage & Osteoarthritis.....	10
Signalling pathways in healthy and hypertrophic chondrocytes .....	11
VHH.....	13
Cartilage culture models .....	14
Next generation <i>ex vivo</i> osteochondral culture model.....	15
Cartilage histopathology assessment.....	15
Goal .....	17
Materials and Methods .....	18
Cell culture and isolation.....	18
Total RNA extraction and quantitative polymerase chain reaction .....	18
Osteochondral plug culture.....	18
Long term culture analysis .....	18
Decalcification method analysis.....	19
Human OA characterization .....	19
Histological analysis.....	19
Hematoxylin & Eosin .....	19
Alcian Blue .....	20
Safranin O.....	20
Immunohistochemistry .....	20
Image analysis .....	20
Transfection and reporter assay .....	21
ELISA binding affinity determination.....	21
Dot blot.....	21
Statistical analysis.....	21
Results .....	22
Experimental set-up characterization .....	22
Isolated bChs are suitable for control experiments .....	22
Osteochondral plugs can be cultured stably for at least 28 days .....	23
Kristensen's is the most optimal decalcification solution .....	24
OA causes decreased cartilage thickness and increased cell density, cell size and number of clusters .....	26
DKK1 and FRZB biological activity .....	30
DKK1 and FRZB neutralize WNT3a activity.....	30

Anti-DKK1 and anti-FRZB VHH biological activity and binding characteristics.....	30
Anti-DKK1 and anti-FRZB VHHs do not neutralize DKK1 and FRZB activity.....	30
Anti-DKK1 VHH binds strongly to rhDKK1, anti-FRZB VHH binds very weakly to rhFRZB .....	31
Anti-DKK1 and anti-FRZB VHHs bind to bCh cell lysate, but not to rhDKK1 or rhFRZB.....	31
Discussion.....	33
Experimental set-up characterization.....	33
Isolated bChs for control experiments.....	33
Long-term culture of bovine osteochondral plugs.....	33
The optimal decalcification method.....	34
Healthy and OA articular cartilage characterization .....	35
DKK1 and FRZB biological activity .....	37
Anti-DKK1 and anti-FRZB VHH biological activity and binding characteristics.....	37
Conclusion .....	40
Recommendations .....	40
References.....	41
Supplementary information .....	50
Supplement 1: Primer sequences.....	50
Supplement 2: Long term culture ability Alcian Blue and H&E staining .....	50
Supplement 3: Decalcification method analysis Alcian Blue and H&E staining .....	51

## Table of definitions

ACAN:	Aggrecan
ACI:	Autologous chondrocyte implantation
ALPL:	Alkaline phosphatase
APC:	Adenomatous polyposis coli protein
AsAP:	Ascorbic Acid 2-phosphate
AXIN:	Axis inhibitor
bChs:	Bovine chondrocytes
BIO:	Glycogen synthase kinase-3 inhibitor 6-bromoindirubin-3-oxim
BMP:	Bone morphogenetic protein
COL2a1:	Collagen 2a1
DKK1:	Dickkopf-1 homolog
DZC:	Deep zone chondrocytes
ECM:	Extracellular matrix
EDTA:	Ethylenediaminetetraacetic acid
ELISA:	Enzyme-linked immunosorbent assay
FBS:	Fetal bovine serum
FRZB:	Frizzled-related protein
GSK3 $\beta$ :	Glycogen synthase kinase 3 $\beta$
hChs:	Human chondrocytes
IHH:	Indian Hedgehog
LEF:	Lymphoid enhancer binding protein
LRP5/6:	Low density lipoprotein receptor related protein
MMP13:	Metalloproteinase 13
MSC:	Mesenchymal stem cell
MZC:	Middle zone chondrocytes
NEAA:	Non-essential amino acids
OA:	Osteoarthritis
PBS:	Phosphate-buffered saline
Pen/strep:	100 U/ml penicillin and 100 $\mu$ g/ml streptomycin

Rh: Recombinant human  
RUNX2: Runt-related transcription factor 2  
SOX9: SRY-Box Transcription Factor 9  
SZC: Superficial zone chondrocytes  
TBS-T: Tris-buffered saline-tween  
TCF: T cell-specific factor  
VHH: Variable heavy chain of the heavy chain only antibody  
WNT: Wingless-Type MMTV Integration Site Family  
WNT3a: WNT Family Member 3A

## Introduction

Osteoarthritis (OA) is the most common joint disorder in the United States, affecting a large population [1]. The disease involves the disruption of the joint articular cartilage, resulting in pain, stiffness, swelling and impaired mobility. OA has a multifactorial aetiology often described as a product of an interplay between systemic and local factors. The prevalence and incidence of OA is expected to increase even more in the future due to an ageing population. It is expected that about 40% of men and 47% of women will develop knee OA in their lifetime, as a consequence of cumulative exposure to risk factors and biological changes. The rapid increase of OA prevalence suggests a rising impact of OA on health care and society [2][3]. Health care costs associated with the treatment of OA can become substantial [4].

Due to the fact that articular cartilage has a poor self-healing capacity, OA is a challenging disease with limited treatment options of which none is a definite cure. Traditionally, pharmacological therapies anti-inflammatory drugs and opioids are prescribed for the relieve of pain [5]. Unfortunately, these drugs are incapable of reversing cartilage damage and go hand-in-hand with side effects [6]. Over the years, regenerative therapies have emerged with the potential to enhance cartilage repair. Current treatments of cartilage defects involve micro-fractures, abrasions, autologous chondrocyte implantation (ACI) and mesenchymal stem cell (MSC) differentiation and implantation. These treatments all involve a regenerative response by the host leading to symptomatic relief. Furthermore, they delay the need for total joint replacement, making them especially plausible treatments for young OA patients [7]. However, the regenerative capacity of cartilage is limited, resulting in incomplete healing and ongoing degradative processes [6][8][9].

Undesirable chondrocyte hypertrophy and terminal differentiation cause matrix degeneration and calcification and are reasons for incomplete healing of the articular cartilage covering the surface of the joint [10][11]. Maintaining the chondrogenic phenotype and avoiding hypertrophy remain a big challenge in cell-based therapeutic strategies [12]. Successful perseverance of articular cartilage is accomplished by the close interaction of several signal transduction pathways [13]. One of them is the Wingless-Type MMTV Integration Site Family (WNT)/ $\beta$ -catenin signalling pathway, which plays a pivotal role in maintaining healthy articular cartilage [14]. Upregulation of the WNT/ $\beta$ -catenin pathway results in the destruction of cartilage due to hypertrophic differentiation, leading to an OA-like phenotype [15]. On the other hand, the downregulation of the WNT/ $\beta$ -catenin pathway results in cartilage destruction due to apoptosis [16]. This stresses the importance of a strict regulation of the WNT/ $\beta$ -catenin signalling pathway. Unfortunately, the exact mechanisms regulating WNT/ $\beta$ -catenin activity, which ensures the chondrogenic phenotype in human, are yet unknown, bringing a halt to the development of novel therapeutic strategies targeting OA [17].

Targeting signalling pathways holds great potential for the development of therapies for OA. However, to overcome the current gap of knowledge, we need to gain insight in the regulation of those signalling pathways in the early stage of OA development. Dickkopf-1 homolog (DKK1) and Frizzled-related protein (FRZB) proteins have been identified as WNT pathway antagonists and are thought to play a significant role in the pathogenesis of OA after injury [18][19]. It is hypothesized that a decrease in the presence of those proteins increase the WNT/ $\beta$ -catenin activity, resulting in hypertrophic differentiation [17]. However, this has not been proven yet on healthy cartilage. In this project, we therefore aim to investigate if anti-DKK1 and anti-FRZB VHH antibodies are able to induce OA in healthy bovine and human cartilage explants to gain insight in WNT pathway signal transduction in the early stage of OA.

## Articular Cartilage & Osteoarthritis

Articular cartilage is a type of hyaline cartilage, which covers the ends of the bones. It makes sure the bones of a joint can move smoothly and without friction. Articular cartilage is an avascular and aneural tissue [20]. It consists for a large part of extracellular matrix (ECM) and for only 5% of chondrocytes [21]. Articular cartilage comprises four distinct regions (figure 1): (1) the superficial tangential zone, (2) the middle zone, (3) the deep zone and (4) the calcified cartilage zone. The last and deepest zone is located immediately above the subchondral bone. The cell morphology and matrix composition is distinct per region. The chondrocytes are small and flat, and the ECM is composed of thin collagen fibrils oriented in a tangential array in the superficial zone. The middle zone comprises the largest part of the articular cartilage and is accountable for 40%-60% of the weight. Chondrocytes are round and are surrounded by radial bundles of thick collagen fibrils in this zone. The same radial bundles are present in the deep zone. The chondrocytes in the deep zone are grouped in columns or clusters [22]. Generally, the cell volume increases from the superficial to the deep zone, while the cell density is reduced. Differences in the morphology of superficial (SZC), middle (MZC) and deep (DZC) chondrocytes are a consequence of the differences in their mechanical milieu [8][23][24]

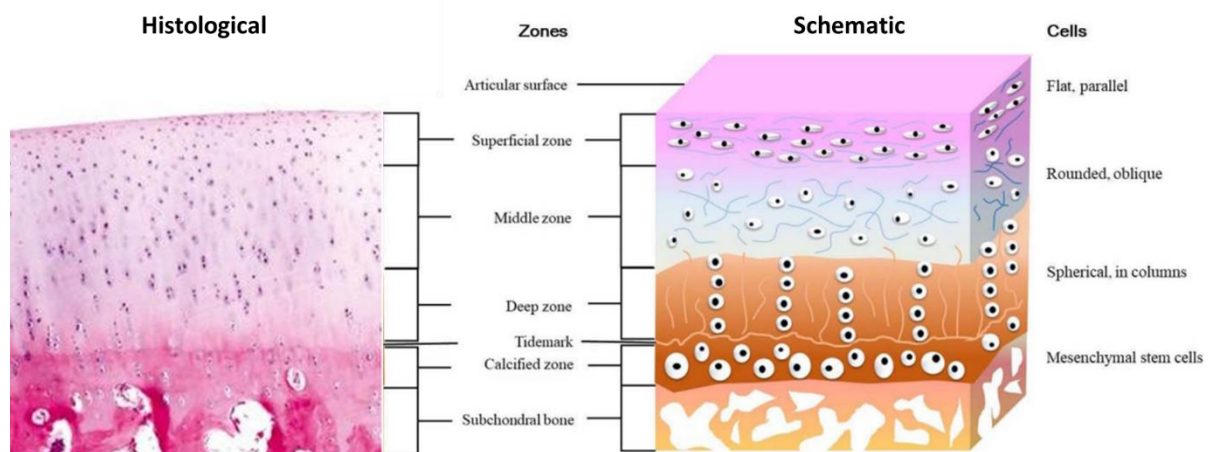


Figure 1: Histological and schematic visualisation of articular cartilage zoning. The cell morphology and matrix orientation is distinct per region and a consequence of the mechanical milieu [25][26].

Since articular cartilage is avascular and aneural, it has low regenerative capabilities. Nevertheless, the tissue is highly susceptible to injury and wear and tear over time due its load-bearing function. If damaged articular cartilage is left untreated, it starts to affect surrounding tissue and ultimately degenerates into OA [27]. During OA the metabolic balance of the chondrocytes is disturbed, resulting in the loss of collagen, mainly collagen type II, and proteoglycans thereby impairing the biomechanical properties of the cartilage [20][28]. During progression of the disease, the chondrocytes start to over-express matrix-degrading enzymes, such as metalloproteinase 13 (MMP13), which exacerbate the breakdown of the ECM [29]. In addition, chondrocytes in the more superficial layers tend to form clusters, while the chondrocytes in the deeper layers undergo apoptosis [30][31]. Overall, the biochemical and biomechanical changes caused by excessive load or injury together contribute to the pathogenesis of OA as can be seen in figure 2 [6][24].

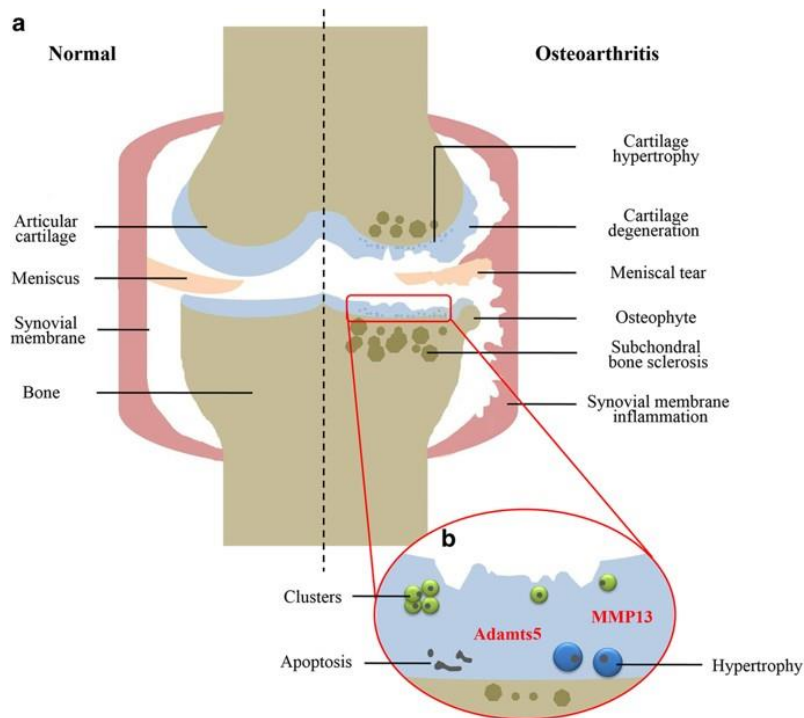


Figure 2: A comparison of a healthy and an OA knee joint. (a) The articular cartilage covers the bone and forms a smooth surface on the bone of the healthy joint. In the OA joint the cartilage is damaged and degenerates. Other structures in the joint are also affected. (b) MMP 13 degrades collagen, chondrocytes in the superficial zone form clusters and chondrocytes in the deep zone undergo apoptosis [107].

Healthy articular cartilage is largely resistant to hypertrophic differentiation. In contrast, growth plate cartilage, another type of hyaline cartilage, naturally undergoes hypertrophic differentiation during the elongation of bones in a process known as endochondral ossification [18]. During endochondral ossification, chondrocytes proliferate, undergo hypertrophic differentiation and die in the end. Afterwards, the ECM constructed is invaded by blood vessels, osteoclasts, bone marrow cells and osteoblasts. The osteoblasts are responsible for the deposition of bone on remnants of the ECM. The changes in chondrocyte behaviour are regulated by systemic and locally secreted factors. These factors act on receptors, which regulate signal transduction pathways and therefore the activation of transcription factors [32][33]. During the progression of OA in articular cartilage, a similar process is observed, at least in a subset of patients, due to an imbalance in extrinsic factors that normally prevent chondrocytes from hypertrophic differentiation [6][29].

### Signalling pathways in healthy and hypertrophic chondrocytes

It has been shown that deregulated hypertrophic differentiation of articular chondrocytes might be a driving factor in the onset of OA. Several signalling pathways are involved in the regulation of hypertrophic differentiation. Pathways involved include the WNT/ $\beta$ -catenin [34][35][36], bone morphogenetic protein (BMP) [37], Indian Hedgehog (IHH) [38] and hypoxia-induced [39] signalling pathways. A disturbance in the natural balance of these pathways leads to the activation or inhibition of one or multiple of these pathways and releases the breaks on hypertrophic differentiation. A small imbalance, such as biomechanical stimulation, can induce a catabolic shift [18] resulting in chondrocytes losing their stable phenotype and starting to express Runt-related transcription factor 2 (RUNX2), Collagen type X, MMP13, IHH and Alkaline Phosphatase (ALPL) (figure 3) [40].

Healthy articular cartilage expresses SRY-Box Transcription Factor 9 (*SOX9*), aggrecan (*ACAN*) and collagen 2a1 (*COL2A1*) (figure 3), and has a mechanism which protects it from undergoing hypertrophic differentiation [41]. It secretes soluble factors inhibiting hypertrophic differentiation of growth plate cartilage [42]. Recently, DKK1 and FRZB have been identified as prime candidates of being these inhibitors [17][18][19]. DKK1 and FRZB are antagonist of the WNT/ $\beta$ -catenin signalling pathway, an important pathway keeping cartilage homeostasis.

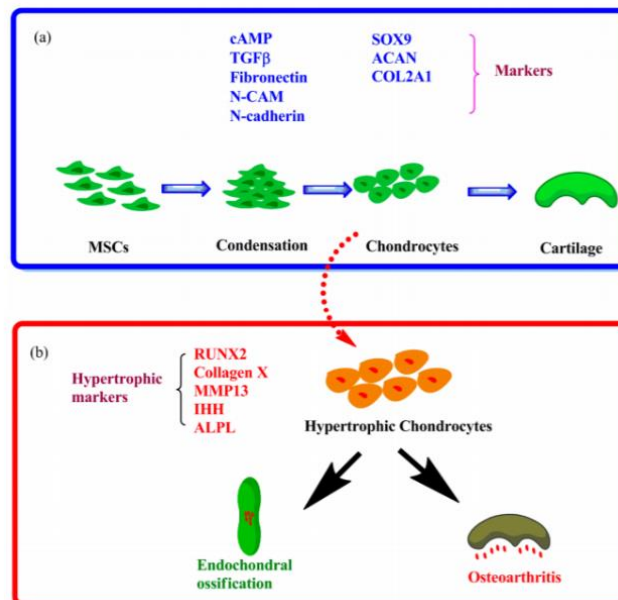


Figure 3: Chondrogenesis of MSCs and hypertrophic differentiation. (a) Chondrogenesis is initiated by the condensation of MSCs. Chondrocytes start to express chondrogenic genes: *SOX9*, *ACAN* and *COL2A1*. Mature chondrocytes secrete matrix components forming cartilage tissue. (b) When chondrocytes undergo hypertrophic differentiation, cell volume increases and *RUNX2*, *Collagen X*, *MMP13*, *IHH* and *ALPL* are expressed. Hypertrophic differentiation can result in either endochondral ossification or OA [17].

The WNT/ $\beta$ -catenin signalling pathway has a strong correlation with chondrocyte hypertrophy and is mediated by a cascade of events as shown in figure 4. In most cases, WNTs bind to the WNT receptor Frizzled, which results in the formation of a complex of Adenomatous polyposis coli protein (APC), Glycogen synthase kinase 3 $\beta$  (GSK3 $\beta$ ) and Axis inhibitor (AXIN). This consequently leads to the release of  $\beta$ -catenin from the complex after which  $\beta$ -catenin accumulates in the cytoplasm and translocates to the nucleus. In the nucleus,  $\beta$ -catenin forms a complex with T cell-specific factor (TCF)/lymphoid enhancer binding protein (LEF) transcription factor to activate target gene transcription. The pathway is activated. However, in absence of any WNT ligand or in presence of WNT inhibitors,  $\beta$ -catenin is destroyed through the phosphorylation of the destruction complex, subsequent ubiquitinylation and targeting for proteasomal degradation [43][40]. A high WNT/ $\beta$ -catenin activity is associated with increased hypertrophic differentiation [44], while maintaining a moderate WNT/ $\beta$ -catenin activity is essential to maintain a chondrogenic phenotype [45].

WNT/ $\beta$ -catenin antagonists DKK1 and FRZB are naturally highly enriched in human articular cartilage. Both proteins can block the pathway activity through a different mechanism. DKK1 blocks WNT/ $\beta$ -catenin signalling through binding to the low density lipoprotein receptor related protein (LRP5/6), which prevents all WNT binding to the co-receptor [46]. FRZB directly binds to WNT proteins blocking the activation of the Frizzled receptor [40]. DKK1 and FRZB are functionally redundant since both of them can inhibit WNT/ $\beta$ -catenin signalling, one can compensate for the loss of the other [19].

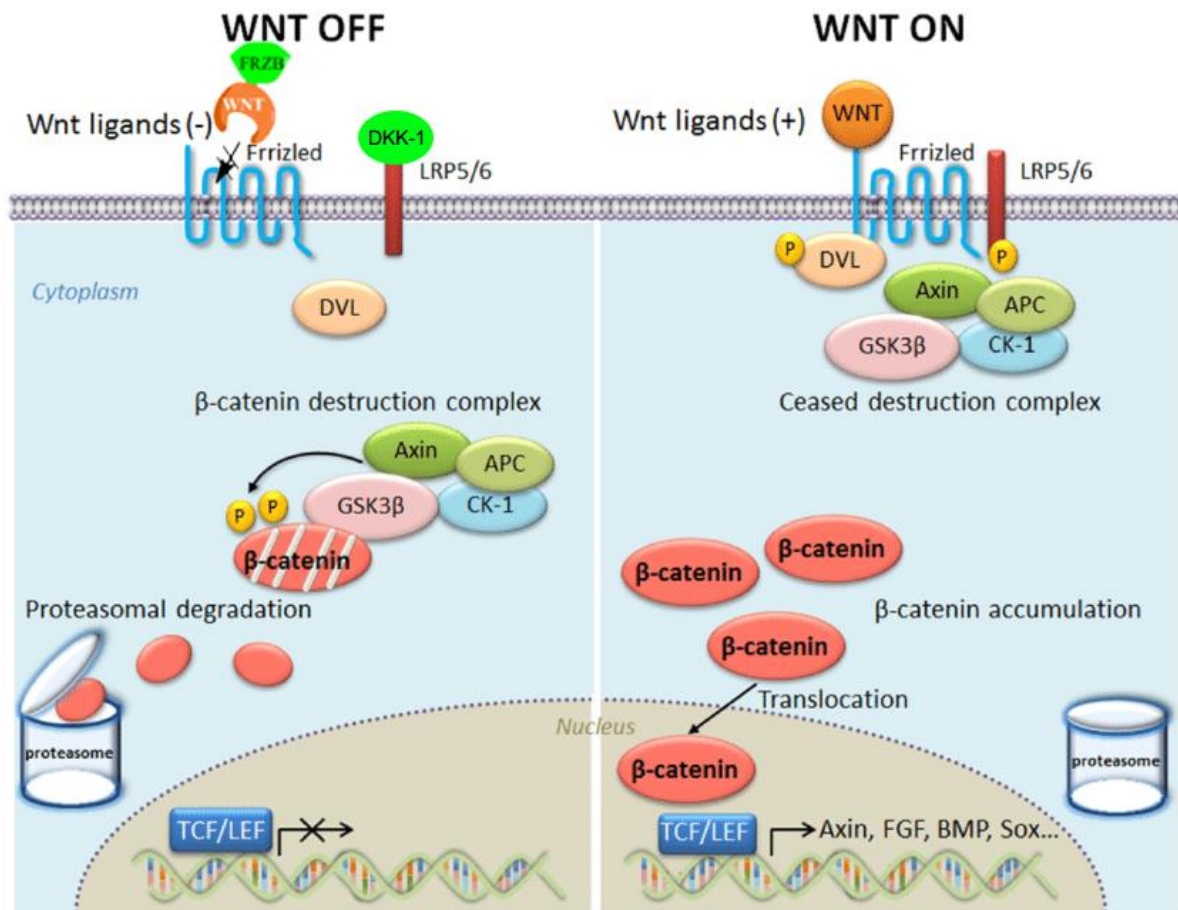


Figure 4: Overview of WNT/ $\beta$ -catenin signalling. When FRZB and DKK1 block WNT/ $\beta$ -catenin signalling, the  $\beta$ -catenin destruction complex phosphorylates  $\beta$ -catenin. The phosphorylated  $\beta$ -catenin is recognized and degraded by proteasomes. When there is no FRZB and DKK1, WNT/ $\beta$ -catenin signalling is turned on. The destruction complex is inhibited and  $\beta$ -catenin accumulates in the cytoplasm after which it translocates to the nucleus where it activates WNT target genes [17].

## VHH

Theoretically, it should be possible to induce OA-like features as hypertrophic differentiation in healthy articular cartilage by the removal of DKK1 and FRZB from the tissue. This could give more insight in the exact mechanisms of the pathogenesis of OA. Captivating the proteins from the tissue can be achieved by a special class of antibodies expressed by the Camelidae family. They are devoid of light chains and are called heavy chain only antibodies. The antigen-binding domain of such special antibody is called variable heavy chain of the heavy chain only antibody (VHH) (figure 5) [47][48]. VHH are unique since they are very small ( $\sim 15$  kDa) and capable of binding with high affinity and specificity to epitopes of the antigen. In addition, they are easy to clone and only consist of a single gene, which means they can be genetically modified to be able to bind to an antigen of choice. A large number of VHH can be obtained by recombinant production in bacteria and yeast [49][50]. All these genetic and structural features make them suitable for the widespread application in research and therapies [51]. In this research, VHH will play an important role in the neutralization of growth factors [52].

To obtain specific VHH, active immunization of llamas or dromedaries is used to isolate VHH with affinities in the nanomolar or picomolar range for the specific antigen. The mRNA of the animal is collected and converted into cDNA. The cDNA is amplified by PCR and digested to isolate the VHH genes. The genes are inserted into a phage-display plasmid. Consequently, a library of phagemids is obtained, which is panned for the desired VHH. After this process shown in figure 6, a single phage is isolated containing the genetic information of the VHH [52][53][54][55].

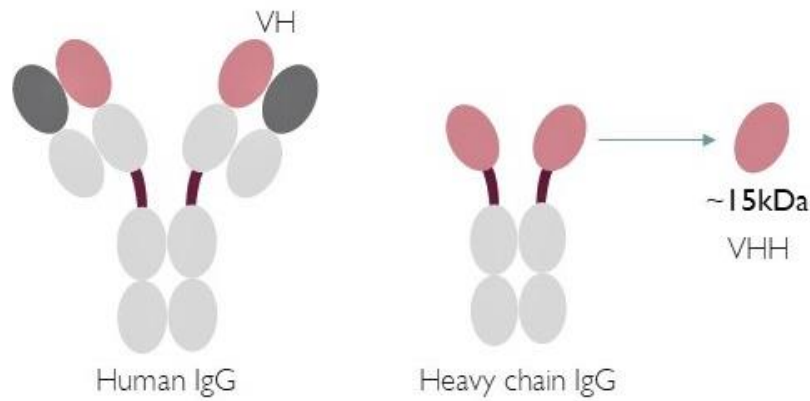


Figure 5: A Camelid antibody only has a heavy chain, while a human antibody has both a light and heavy chain. A VHH constitutes the variable heavy chain of the heavy chain only antibody [17].

Using this method, Zhong et al. selected VHH against DKK1 and FRZB from nonimmune llama VHH-phage display libraries [17]. A definite choice of anti-DKK1 and anti-FRZB VHH was made after testing the functionality. H7 proved to be the most effective in blocking DKK1, while TSF-1F7 proved to be the most effective in blocking FRZB. The optimum concentration was set at a concentration of 5  $\mu\text{g/ml}$ . Therefore, these VHH are used in this research.

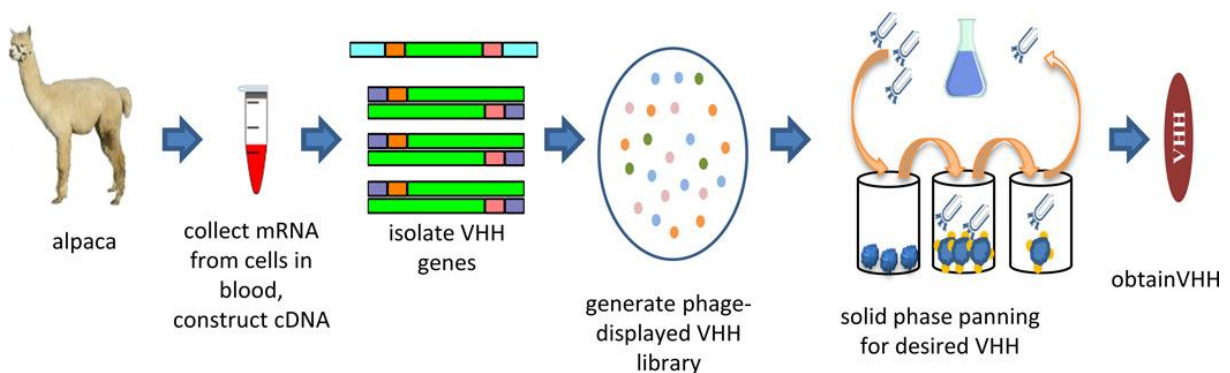


Figure 6: Overview of the selection of specific VHH for an antigen. Members from the Camelid family are actively immunized. mRNA is isolated from the animal, converted into cDNA, amplified and digested. The obtained VHH genes are displayed in phages, creating a library. The library is panned for desired VHH [17].

### Cartilage culture models

Several *in vitro* cartilage culture models are used to better understand the biological processes *in vivo*, including the pathogenesis of OA. These models include monolayer culture, pellet culture, scaffold culture [56][57] and explant culture. The first one is a two-dimensional culture method, usually the easiest one, where chondrocytes are cultured on the flat surface of a culture flask. However, this method lacks the interaction with the surrounding elements of the three-dimensional (3D) situation *in vivo*, which can make it behave differently. On the other hand, pellet and scaffold cultures do provide the cells with a suitable 3D environment to secrete and build a new ECM. Nevertheless, this newly built matrix may make chondrocytes act differently from those in naturally occurring ECM [58].

Therefore, explant culture is thought to be the most advantageous. Since the explant is directly harvested from the host, explant culture should better keep the morphological and biosynthetic characteristics of cartilage *in vivo* [59]. In addition, it cancels out the complicated systematic parameters *in vivo* [60]. It should, however, not be forgotten that extraction of the cartilage subjects the explant to mechanical trauma, which can have an effect on its metabolism [21].

To investigate the effect of capturing DKK1 and FRZB from a cartilage tissue on the development of OA-like symptoms, Zhong et al. used a pellet co-culture of hMSCs and human chondrocytes (hChs) [17]. The results partially proved the hypothesis of DKK1 and FRZB playing a crucial role in the pathogenesis of OA. Nevertheless, the hChs used for this experiment were healthy-looking/preserved hChs, but from an OA knee. It is thought that the cytokines coming free during the inflammatory reaction, might have had an effect on the behaviour of the hChs in the pellet co-culture of the experiment. This stresses the importance of healthy defined culture. Therefore, the same hypothesis will be evaluated, but this time healthy cartilage explants will be used from cows. This brings along other difficulties, such as anatomical differences and handling [21].

#### Next generation *ex vivo* osteochondral culture model

Over the years, cartilage-only models have been useful for gaining insight into cartilage behaviour and disease pathogenesis. However, the absence of bone is an inherent limitation for preclinical research. It has been reported that cartilage-only models show a significant decrease in cartilage-related gene expression [61]. Therefore, *ex vivo* osteochondral models have been developed, in which cartilage with its underlying bone is cultured in cartilage medium. Unfortunately, the model is not suitable for culture times over 28 days, since the expression of cartilage-related genes decreases. It is thought that this decrease may be caused by secreted factors from the subchondral bone, which also serves as nutrient supply for the cartilage [62][63]. Therefore, Schwab et al. developed a model with two compartments, which separates bone-specific medium from cartilage-specific medium [64]. This new generation model represents the *in vivo* model more accurately. They proved that cartilage and bone phenotype are maintained for a culture period of at least 56 days making it a highly relevant new platform to study cartilage behaviour and disease pathogenesis [64][65][66].

#### Cartilage histopathology assessment

A standardized and reliable histopathological assessment of cartilage degeneration is important in clinical practice and research. It is the basis of selecting healthy cartilage and comparing the outcome of different research conditions. Therefore, the assessment of OA histopathology has been standardized and is called the OARSI grading system [67][68]. The OARSI grading system consists of six grades, from grade 0, no involvement, to grade 6, deformation. Increasing grade indicates a higher severity and biological progression of the disease. The involvement of a deeper layer of cartilage indicates a more advanced disease. Pritzker et al. described all stages in detail and can be used as reference for grading the cartilage during this research [67]. A histological assessment of grade 0 to 5 is shown in figure 7. Furthermore, the stage is another parameter of OA progression [69]. It defines the horizontal extent of the cartilage involved in the disease and is usually expressed as a percentage of the total cartilage on the surface of the joint [67].

In addition to the OARSI grading system, biomechanical properties could be used to find the stage of OA of a cartilage sample. It has been found that the dynamic modulus significantly decreases from grade 0 to grade 4. Furthermore, the aggregate modulus can be used to differentiate between grade 0, grade 1 and grade 2. Progression of OA involves the reduced ability to withstand compressive loads [69].

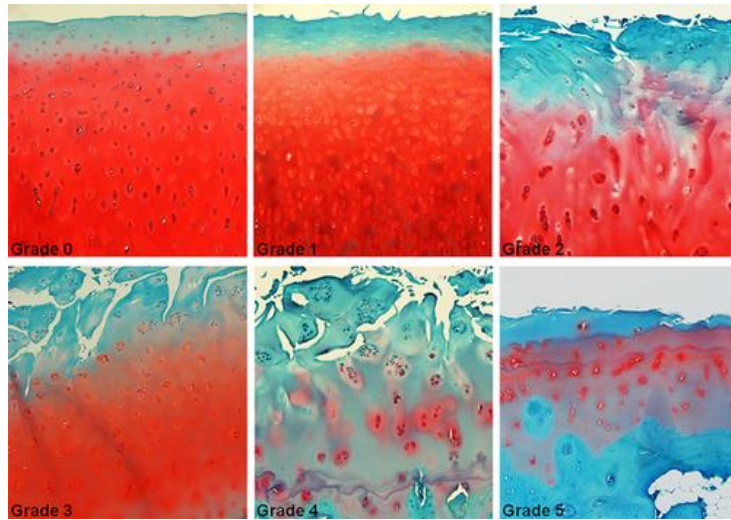


Figure 7: Visualization of histological characteristics of grade 0-5 of the OARSI grading system. Grade 0: No OA, Grade 1: Surface intact, Grade 2: Surface discontinuity, Grade 3: Vertical fissures, Grade 4: Erosion and Grade 5: Denudation. Grade 6 is not shown, but involves deformation of the cartilage contour and bone remodelling [52].

## Goal

The aim of this research is to investigate if anti-DKK1 and anti-FRZB VHH antibodies are able to induce osteoarthritis-like symptoms in healthy bovine and ultimately human cartilage explants. The main research question is: ***'Are anti-DKK1 and anti-FRZB VHH antibodies able to induce OA in healthy bovine osteochondral plugs?'***

It has already been proven that the addition of anti-DKK1 and anti-FRZB VHH antibodies can neutralize human DKK1 and FRZB inhibition measured by restored WNT signalling [17]. However, these findings are still preliminary due to the lack of healthy cartilage explants. Therefore, we will investigate whether these VHHs can neutralize bovine DKK1 and FRZB and if that results in osteoarthritic-like symptoms in healthy bovine osteochondral plugs.

To achieve this, the research has been divided into three parts with each its individual question:

1. What is the biological activity of DKK1 and FRZB?
2. What is the biological activity of anti-DKK1 and anti-FRZB VHH?
3. Does blocking DKK1 and FRZB activity in bovine osteochondral plugs result in morphological osteoarthritic-like changes?

First of all, the biological activity of DKK1 and FRZB will be evaluated using a luciferase assay. The second part elaborates on this and should answer the question if anti-DKK1 and anti-FRZB VHHs can block DKK1 and FRZB thereby neutralize their activity. The same luciferase assay set-up will be used. Once the VHHs have been proven to be neutralizing, the ability of anti-DKK1 and anti-FRZB to induce OA in healthy bovine osteochondral plugs can be evaluated. Before this third and main question can be answered, some experimental conditions need to be established. Therefore, isolated bovine chondrocytes (bChs) will be characterized, long-term culture ability tested, the best decalcification technique determined and OA in human osteochondral plugs characterized.

## Materials and Methods

### Cell culture and isolation

C2C12 cells, immortalized mouse myoblasts, were cultured routinely in tissue culture polystyrene flasks (ThermoFisher Scientific) at 37°C under 5% CO<sub>2</sub> atmosphere. The culture medium used for C2C12 cells was DMEM (1x) (Gibco) containing 10% fetal bovine serum (FBS) (Gibco) and 100 U/ml penicillin and 100 µg/ml streptomycin (1% pen-strep) (Gibco). Cells were passaged every 3 to 4 days using 0.25% trypsin/EDTA (Gibco).

To provide a control for the experiments with osteochondral plugs, bChs were obtained from healthy bovine full thickness cartilage, dissected from knee biopsies of a slaughtered cow of unknown age. To isolate the cells, the cartilage was cut in small pieces and digested in DMEM containing 10% FBS, 10% collagenase type II (Gibco) and 1% pen/strep for 16-20h. Subsequently, the bChs were expanded at a density of 5,000 cells/cm<sup>2</sup> in chondrocyte medium containing DMEM, 10% heat-inactivated FBS, 20 mM Ascorbic Acid 2-phosphate (AsAP) (Gibco), 0.4 mM proline (Gibco), 1x non-essential amino acids (NEAA) (Gibco) and 1% pen-strep in tissue culture polystyrene flasks at 37°C under 5% CO<sub>2</sub> atmosphere. BChs were passaged every 3 to 4 days using 0.25% trypsin/EDTA (Gibco).

### Total RNA extraction and quantitative polymerase chain reaction

To be able to analyse bCh behaviour upon cellular stimulation, cells were harvested and RNA was isolated using the NucleoSpin RNA II Kit (Macherey-Nagel). The concentration and purity of the RNA samples were determined using the NanoDrop 2000 (ThermoFisher). mRNA was reverse-transcribed into cDNA using the iScript cDNA Synthesis Kit (Bio-Rad). SYBR Green SensiMix (Bioline) was used to perform quantitative polymer chain reaction (qPCR). The qPCR was carried out using the Bio-Rad CFX96 (Bio-Rad) using the following protocol: cDNA denaturation for 10 min at 95°C, followed by 40 cycles consisting of 15 s melting at 95°C, 15 s annealing at 60 °C and 15 s extension at 72°C. The programme ends with a melting curve from 65°C to 95°C (5s/°C). The primer sequences are listed in supplement 1.

### Osteochondral plug culture

#### Long term culture analysis

A bovine knee was collected from the slaughterhouse and dissected to obtain bovine osteochondral plugs to study long term culture stability. Osteochondral plugs with a diameter of 6 mm were isolated from the tibia plateau using a Dremel while cooling with 4°C phosphate-buffered saline (PBS)(Lonza) supplemented with 1% pen/strep. Plugs were stored for a maximum of 4 hours in PBS supplemented with 1% pen/strep before put in culture.

To improve culture stability in terms of osteochondral plug structure and viability, osteochondral plugs were cultured in an *ex vivo* osteochondral culture platform (LifeTec Group BV). This platform consists of a 6-well plate with inserts, which provide a separate culture compartment for bone and cartilage as can be seen in figure 8. The osteochondral plugs were mounted into the inserts using an O-ring positioned exactly at the interface between cartilage and bone. This structure creates two isolated culture compartments. The upper compartment containing the cartilage and the lower compartment containing the bone, each with their respective media. Long term culture in this platform was evaluated.

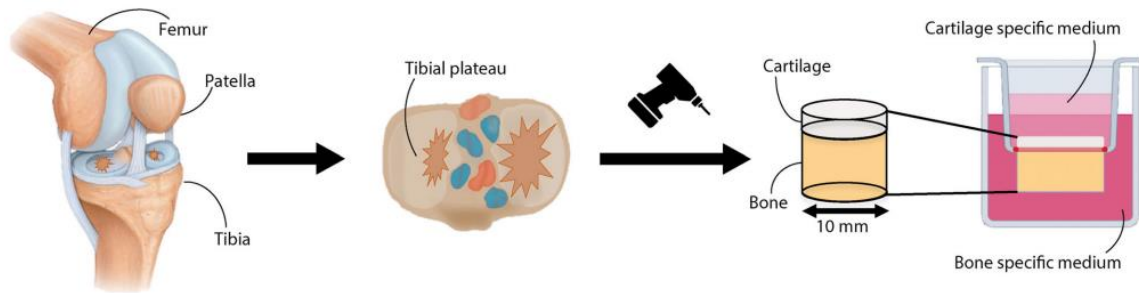


Figure 8: Osteochondral plug harvesting and culturing in the ex vivo osteochondral plug platform. The plugs is inserted in the O-ring, creating a cartilage and a bone compartment [64].

Plugs were cultured for 1, 6, 14, 21 and 28 days in the osteochondral plug culture platform and 28 days in a polystyrene well plate. Two plugs were cultured per condition. Before histological analysis plugs were fixed in 10% phosphate-buffered formalin (pH=7) for 48h at room temperature and decalcified for 18 days in Kristensen's solution containing 16.6% formic acid (Sigma) and 3.4% sodium formate (Sigma) in dH<sub>2</sub>O.

#### Decalcification method analysis

Another bovine knee was collected and dissected as described. Ten plugs were obtained and cultured for 5 days in the osteochondral plug culture platform. After fixation with 10% phosphate-buffered formalin (pH=7) for 48h at room temperature, osteochondral plugs were decalcified. There are a couple of different decalcification methods. Five different decalcification conditions were tested to standardize a decalcification method for further experiments: 12.5% ethylenediaminetetraacetic acid (EDTA) (Sigma) at 4°C, 12.5% EDTA at RT, 20% EDTA at 4°C, Kristensen's solution at 4°C and Kristensen's solution at RT.

#### Human OA characterization

An OA human knee was collected from a patient undergoing a total knee replacement at ZGT (hospital Hengelo). Of the least affected areas of the tibia plateau, 2 macroscopically healthy plugs were isolated. From the highly affected areas of the tibial plateau, 2 macroscopically OA plugs were obtained. The plugs were cultured for 21 days in the osteochondral plug culture platform, after which they were fixed in 10% phosphate-buffered formalin (pH=7) for 48h at room temperature. Plugs were decalcified in 12.5% EDTA for 31 days.

#### Histological analysis

After culture, fixation and decalcification, plugs were dehydrated in the Excelsior tissue processor (ThermoFisher) using a programme of 26h. Immediately after, the osteochondral plugs were embedded in paraffin. Five micrometer thick sections were cut using a microtome (Shandon). Before staining, the slides were dried for 1h at 65°C, deparaffinized in Xylene (VWR) and rehydrated with graded ethanol (Assink Chemie). Tissue slides were stained with Hematoxylin & Eosin (H&E), Alcian Blue or Safranin O. After staining, slides were mounted with GLC™ Mounting Medium (Sakura).

#### Hematoxylin & Eosin

Slides were stained for cell nuclei using Hematoxylin Gill #3 solution (Sigma) for 8-10 min. After differentiation and de-staining in Acid EtOH, washing in running tap water and dehydration using graded ethanol, the slides were stained for extracellular matrix and cytoplasm using alcoholic Eosin-Y solution (Sigma) for 30 s.

## Alcian Blue

Slides (containing 5  $\mu\text{m}$  sections) were stained for sulphated glycosaminoglycans (GAGs) with a 0.5% w/v solution of Alcian Blue (pH=1) (Sigma) for 30 min. A counterstaining with 0.1% w/v nuclear fast red (Sigma) for 5 min was used to visualize cell nuclei.

## Safranin O

Slides were stained with hematoxylin Gill #3 solution for 5 min. Slides were differentiated and de-stained in Acid EtOH, washed in running tap water and dehydrated using graded ethanol. Slides were stained with 0.001% w/v Fast green solution (Sigma) for 3.5 min, quickly rinsed with Acetic Acid for 15 s and stained for sulphated GAGs with 0.1% w/v Safranin O solution (Sigma) for 5-7 minutes.

## Immunohistochemistry

Immunohistochemical staining of collagen type I and collagen type II was performed using 5  $\mu\text{m}$  sections. Slides were dried for 1h at 56°C, deparaffinized in Xylene (VWR) and rehydrated with graded ethanol (Assink Chemie). Slides were preincubated with 0.1% pepsin (Sigma P7000) for 30 min at 37°C. Slides were blocked with 0.3% H<sub>2</sub>O<sub>2</sub>-PBS (Sigma) for 10 min at room temperature (RT) followed by blocking with 5% bovine serum albumin (BSA)-PBS (Sigma) for 30 min at RT. Rabbit polyclonal collagen type I antibody (NB600-408, Novus Biologicals) or collagen type II antibody (ab34712, Abcam) were diluted 1:200 in 5% BSA-PBS and incubated overnight at 4°C. The next day, goat anti-rabbit HRP coupled IgG antibodies (DAKO) 1:100 diluted in 5% BSA-PBS were incubated at the slides for 1h at RT. The target protein was detected using the DAB substrate kit (Abcam) according to manufacturer's protocol for 10 min at RT. Slides were counterstained with hematoxylin Gill #3 for 30 s and mounted with GLC™ Mounting Medium (Sakura). The NanoZoomer (Hamamatsu) was used to image the slides. Controls underwent the same procedure without primary antibody incubation.

## Image analysis

Images obtained from stained slides were analysed using NDP viewer (Hamamatsu) and ImageJ. Staining intensity was determined by inverting the colour image to a black and white image and measuring the grey value of a same sized area and position on the slides. Darker areas are linked to smaller grey values and lighter areas to higher values. In general a decrease in staining intensity, leads to an increase in grey value. Furthermore, several parameters were determined using ImageJ as can be seen in figure 9 and 10. The size of the three cartilage zones, cell size and pericellular matrix size was measured. The amount of cells per area was also determined.

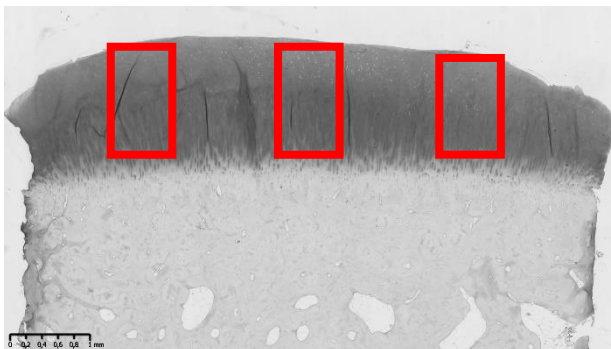


Figure 9: Visualization of the method to determine staining intensity.

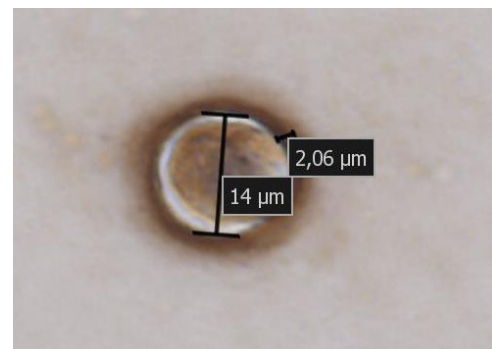


Figure 10: Visualization of the method to measure cellular diameter and pericellular matrix thickness.

### Transfection and reporter assay

C2C12 cells were seeded into a 96-well plate at 10,000 cells/cm<sup>2</sup> and incubated in DMEM supplemented with 10% FBS and 1% pen/strep for one day at 37°C under 5% CO<sub>2</sub>. At day 2 the medium was changed to starvation medium containing DMEM, 1% FBS and 1% pen/strep. Furthermore, the cells were co-transfected with 0.1 µg Super Topflash reporter DNA and 0.005 µg Renilla DNA using lipofectamine 2000 (ThermoFisher) in Opti-MEM (Gibco).

To determine the biological activity of DKK1 and FRZB, the transfected cells were stimulated with a combination of glycogen synthase kinase-3 inhibitor 6-bromoindirubin-3-oxim (BIO), recombinant human WNT family member 3a (rhWNT3a) (R&D systems), rhDKK1 (R&D systems) and rhFRZB (R&D systems) at day 3 for 24 hours. After 24h of stimulation, luciferase activity was determined using Promega Dual-Glo® (Promega E2920). Luciferase activity was corrected for transfection efficiency. To determine the biological activity of anti-DKK1 H7 and anti-FRZB TSF-1F7 VHHs, the transfected cells were stimulated with anti-DKK1 or anti-FRZB VHHs for 1h before combination of rhWNT3a, rhDKK1 and rhFRZB was added.

### ELISA binding affinity determination

To determine the apparent affinity of anti-DKK1 for rhDKK1 and anti-FRZB for rhFRZB, a titration ELISA was performed. Maxisorp well plates (ThermoFisher) were coated with 1 µg rhDKK1 or rhFRZB overnight at 4°C. The next morning 4% Marvel skimmed milk (Campina) in PBS-Tween 0.5% (PBST) (Sigma) was added for 1h of blocking. Next, a concentration range of anti-DKK1 VHHs (0.0001-1,000 nM) or anti-FRZB VHHs (0.0001-10,000 nM) was added to the wells for 1h at RT. After several washing steps with PBST, a primary rabbit anti-VHH (QVQ) antibody diluted 1:1000 in 1% Marvel skimmed milk was incubated for 1h at RT. After several washing steps, a goat anti-rabbit antibody coupled to an HRP, which was diluted 1:1000 in 1% Marvel skimmed milk, was incubated for 1h at RT. Glo substrate A and glo substrate B (Glo substrate reagent pack, R&D systems) were added to the wells 1:1 for 20 min, after which the stop solution (R&D systems) was added. The amount of converted HRP (A 450 nm) was measured with the Multiskan Go (ThermoScientific) and is proportional to the amount of bound VHH.

### Dot blot

Anti-DKK1 and anti-FRZB VHHs were analysed for their ability to bind bovine DKK1 and FRZB. bChs cell lysates were obtained by lysing cells with RIPA buffer (ThermoFisher). As a control, rhDKK1 and rhFRZB were blotted on a dry nitrocellulose membrane (BioRad). Heated and unheated bCh cell lysate were also blotted on a nitrocellulose membrane. Membranes were incubated in 5% Marvel skimmed milk in tris-buffered saline (Sigma)-tween(TBS-T) for 1h at RT. The membrane was then incubated with 1000 nM of anti-DKK1 or anti-FRZB VHHs in 5% Marvel skimmed milk in TBS-T for 1h at RT. After three washes with TBS-T, the membrane was incubated with rabbit anti-lama HRP coupled antibody in 5% Marvel skimmed milk in TBS-T for 1h at RT. The membrane was washed three times. Bound conjugate was visualized with the SuperSignal West Femto maximum sensitivity substrate (ThermoFisher) according to manufacturer's protocol.

### Statistical analysis

Data are expressed as mean ± SD, where at least a triplicate was used. Statistical differences between two conditions were analysed by one-way ANOVA. P<0.05 was considered statistically significant and was indicated with an asterisk.

## Results

### Experimental set-up characterization

Isolated bChs are suitable for control experiments

Bovine chondrocytes were isolated from healthy bovine cartilage explants to act as control for the experiments regarding the osteochondral plugs. Before the cells can be used as control, the cells need to be characterized. To investigate if the cells have an expected response to WNT pathway stimulation, gene expression analysis was performed for *AXIN2*, *ACAN*, *COL2A1* and *COL10A1*. *AXIN2* is a direct target gene of the WNT pathway. *ACAN*, *COL2a1* and *COL10a1* are interesting since they show changes in expression in OA and also through WNT pathway activation [70]. The bChs are stimulated for different times, since gene expression changes over time.

Figure 11 shows that *AXIN2* expression was upregulated upon stimulation with BIO or WNT3a for all time points. The increase in *AXIN2* expression was higher upon stimulation with BIO than with WNT3a. The expression decreased in time after WNT3a stimulation. Furthermore, *ACAN* expression decreased over time for stimulation with BIO. For WNT3a, *ACAN* expression showed a slight decrease at 24h, however, it is not a significant difference compared to the control. For *COL2a1* expression, the decrease was also highest at 24h of stimulation. After 24h, the *COL2a1* expression increased again. Lastly, the expression of *COL10a1* first decreased and then increased upon BIO stimulation. For WNT3a it also seems that *COL10a1* expression increased, however, this is not significant.

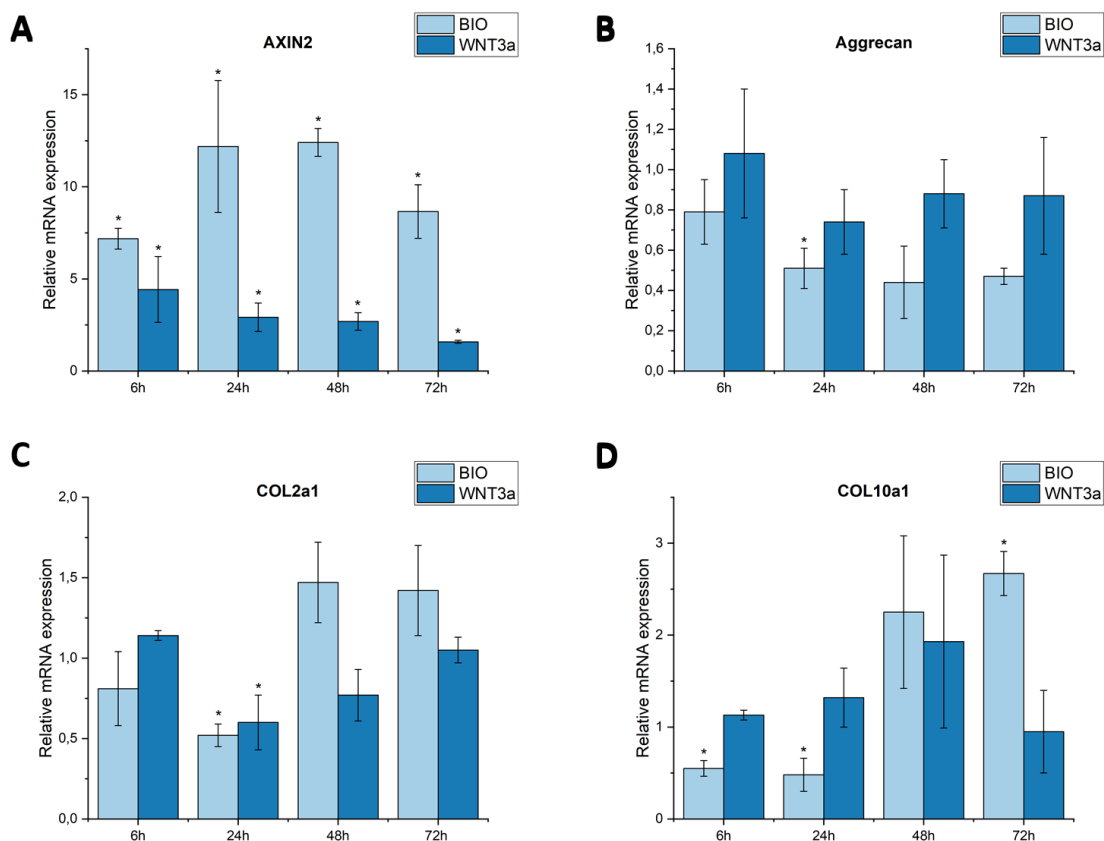


Figure 11: The effect of WNT pathway stimulation with 1  $\mu$ M BIO and 100 ng/ml WNT3a on (A) *AXIN2*, (B) *ACAN*, (C) *COL2a1* and (D) *COL10a1* gene expression. BChs (p8) were cultured in a polystyrene well plate and stimulated for 6h, 24h, 48h and 72h. mRNA expression is relative to the control, which is set at 1, at the same point. The target gene expression was normalized to GAPDH expression. Bars show the mean  $\pm$  SD (n=3). \*p < 0.05 versus control at same time point.

Osteochondral plugs can be cultured stably for at least 28 days

To be able to investigate the effect of anti-DKK1 and anti-FRZB VHHs in culture with bovine osteochondral plugs, the plugs need to be cultured for some time to notice any effect. Therefore, the culture stability, in terms of cartilage viability, matrix tissue content and structure, over a period of 28 days was first investigated. The bovine osteochondral plugs were analysed by Safranin O, Alcian Blue and Hematoxylin & Eosin staining. The culture stability was determined by the staining intensity. It was expected that the osteochondral plugs can be cultured stably for 28 days in the *ex vivo* osteochondral platform [64][66]. In addition, osteochondral plug culture in the *ex vivo* osteochondral platform was compared to culture in a well plate with only cartilage medium. It was expected that culture in the *ex vivo* osteochondral culture platform is more stable than culture in a normal well plate.

Representative images of the Safranin O stained sections are shown in figure 12. The Alcian Blue and the H&E stained sections can be found in supplement 2. The OARSI scores of the cartilage were 0 or 1, since most surfaces were completely smooth or slightly damaged due to the drilling of the plugs. The average thickness of the cartilage was  $1.42 \pm 0.32$  mm, which is average for an adult cow. Culturing the osteochondral plugs in the *ex vivo* osteochondral culture platform did not lead to significant changes in staining intensity over time as can be seen in figure 13A.

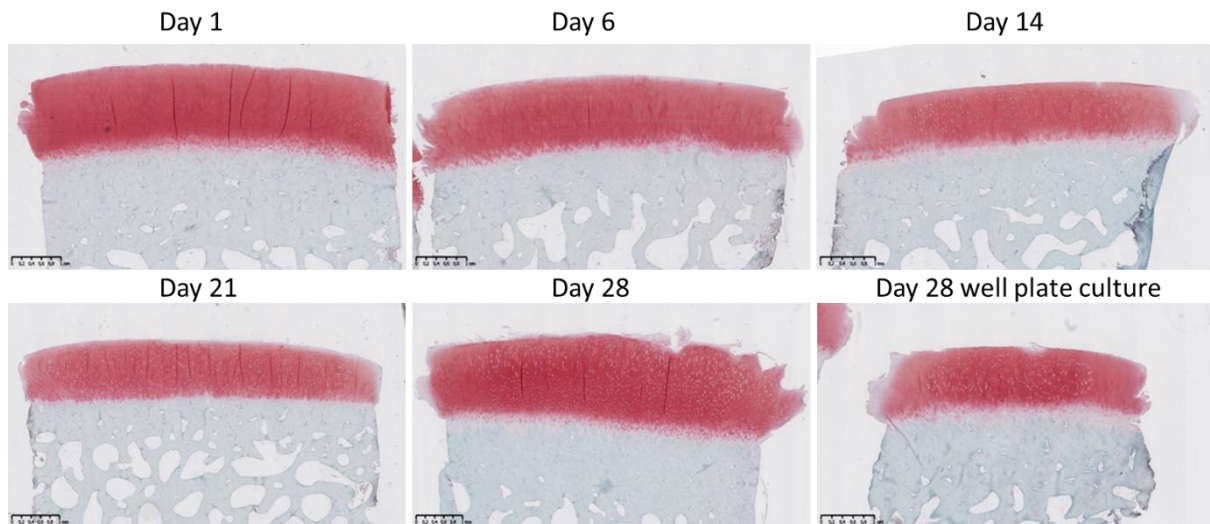


Figure 13 Representative osteochondral plug sections stained with Safranin O. The osteochondral plugs are cultured for 1, 6, 14, 21 and 28 days before they are fixed, decalcified and processed (n=2).

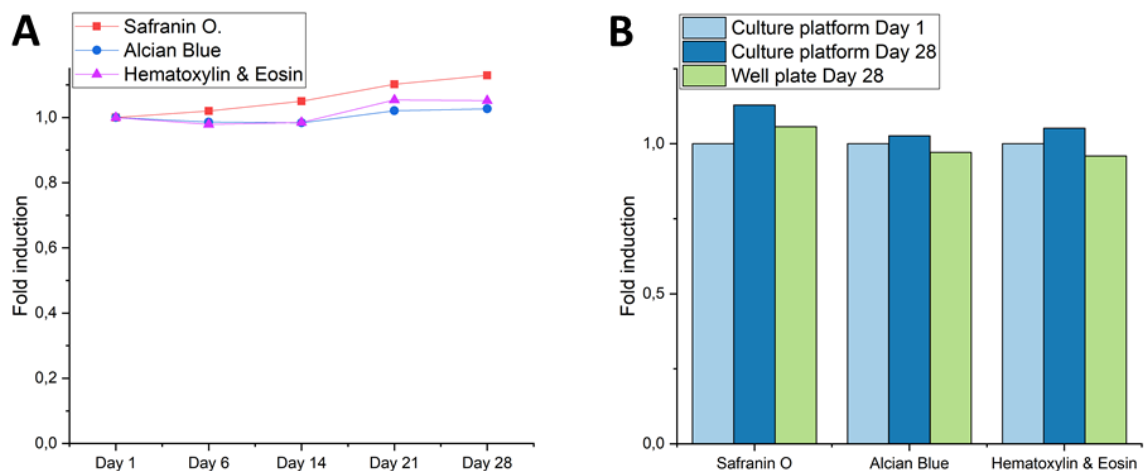


Figure 13: The relative staining intensity of osteochondral plugs cultured in the *ex vivo* osteochondral culture platform expressed as fold induction compared to day 1 (A) over time and (B) compared to normal single compartment well culture. (n=2)

When comparing the *ex vivo* osteochondral culture platform with separate compartments for cartilage and bone to a well plate culture with only cartilage medium, there is again not a significant change in staining intensity (figure 13B). It does look like the normal well plate culture has a lower fold induction than the *ex vivo* osteochondral culture platform culture meaning the grey value was lower for the normal well plate culture and an initially darker red staining was observed, which is related to a higher sulphated GAGs content.

#### Kristensen's is the most optimal decalcification solution

There are several different decalcification methods mentioned in literature of which 12.5% EDTA at 4°C is the standard. However, with plugs with a diameter of 6 mm it can take 4-6 weeks before the bone is fully decalcified. Kristensen's decalcification solution can decalcify the same size plug in 2-3 weeks, which is significantly faster. Nevertheless, Kristensen's is an acid decalcification solution, which can result in damage to the tissue, such as loss of epitopes [71][72]. The temperature also has an influence on the decalcification time and antigenicity conservation. Therefore, an experiment was performed to determine the standard decalcification method for further experiments. The decalcification method was evaluated on time, microscopic morphology preservation and antigenicity conservation. It was expected that the microscopic morphology preservation is good for all decalcification techniques. Furthermore, it was expected that the conditions using Kristensen's will destroy epitopes.

Representative images of the Safranin O stained sections for the different decalcification methods are shown in figure 14. The OARSI score for all sections was 0, meaning that all osteochondral plugs were completely healthy based on structure. The average thickness of the cartilage differed a lot per plug depending on the area of the tibial plateau the plugs came from. The average thickness was  $3.38 \pm 1.38$  mm and therefore it is thought the donor cow for this experiment was younger than the one from the long-term culture evaluation.

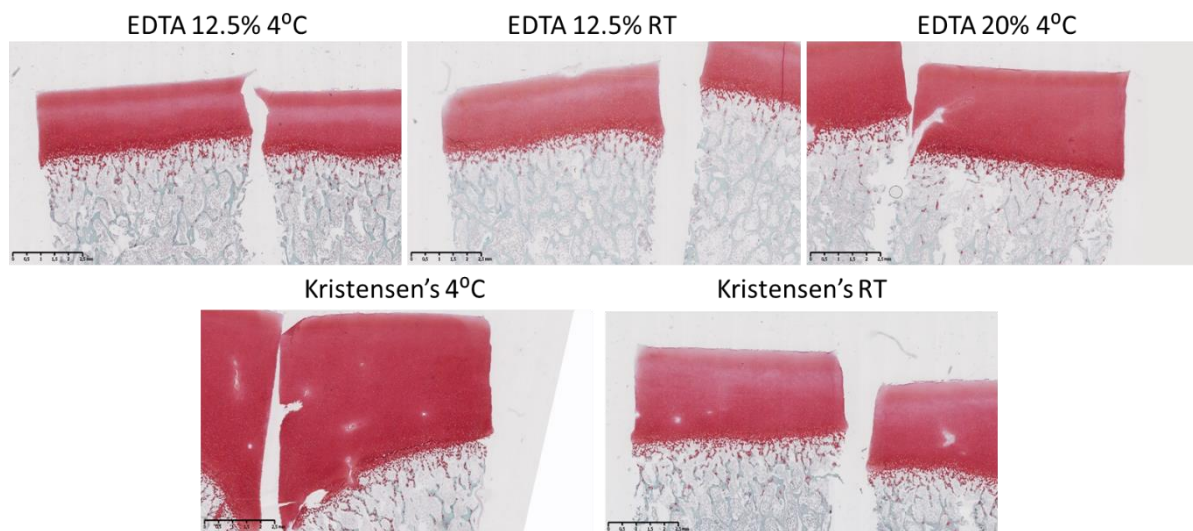


Figure 14: Representative osteochondral plug sections stained with Safranin O. The osteochondral plugs are cultured for 5 days before they are fixed, decalcified and processed. For the decalcification five different methods were used: 12.5% EDTA at 4°C, 12.5% EDTA at RT, 20% EDTA at 4°C, Kristensen's solution at 4°C and Kristensen's solution at RT (n=2).

As can be seen, the cartilage stained red in all images. It looks like there was a slight loss in red staining in the middle zone of the cartilage for the EDTA 12.5% at 4°C, EDTA 12.5% at RT and Kristensen's at RT. However, the average staining intensity over the superficial, middle and deep zone did not change significantly between the different decalcification methods as shown in figure 15.

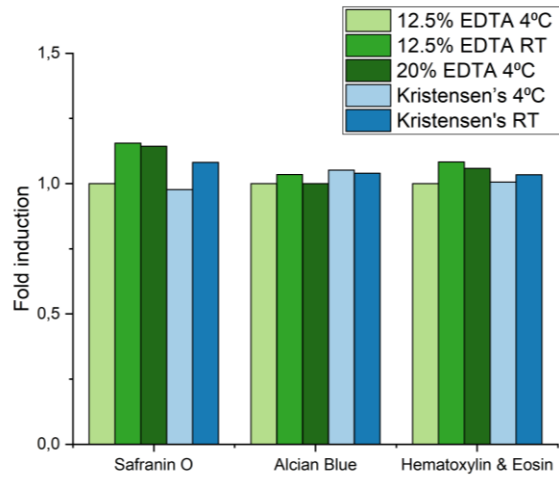


Figure 15: The relative staining intensity of osteochondral plugs cultured decalcified with different decalcification methods expressed as fold induction. (n=2)

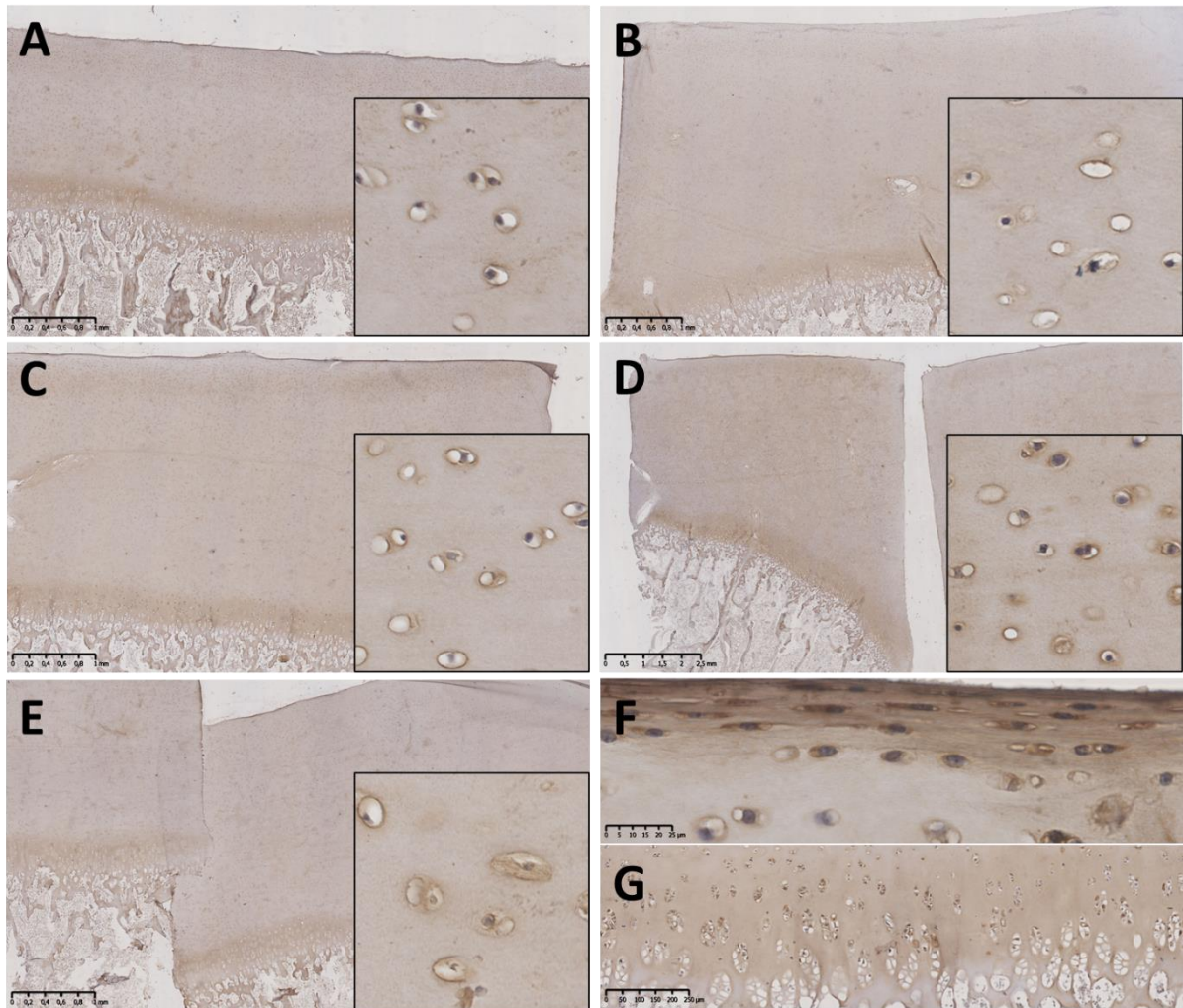


Figure 16: Representative osteochondral plug sections subjected to different decalcification methods stained for collagen II: (A) 12.5% EDTA at 4°C, (B) 12.5% EDTA at RT, (C) 20% EDTA at 4°C, (D) Kristensen's solution at 4°C and (E) Kristensen's solution at RT, (n=2). Collagen II is located mainly around the cells in the pericellular matrix, (F) in the superficial zone and (G) around the tideline.

The antigenicity conservation was investigated by performing an immunohistochemical (IHC) staining on the sections. If the epitopes are destroyed by the decalcification method, the paratope of the antibody cannot bind and no specific staining can be seen. Representative images of the collagen II staining are shown in figure 16. Collagen II was stained in all sections for all different decalcification methods. Collagen II was located in the pericellular matrix around the cells, in the superficial zone and in the hypertrophic zone as shown in figures 16E and F.

The last point of evaluation was the time it takes for an osteochondral plug to decalcify for the decalcification methods. The microscopic morphology preservation and antigenicity conservation were both very good for all different methods. However, there was big difference in time it took to decalcify. As can be seen in table 1, Kristensen's took 18 days, while 12.5% and 20% EDTA at 4°C took 33 days. At RT, 12.5% EDTA decalcified slightly faster.

*Table 1: Summary of the decalcification method evaluation on time, microscopic morphology preservation and antigenicity conservation.*

	<b>12.5% EDTA 4°C</b>	<b>12.5% EDTA RT</b>	<b>20% EDTA 4°C</b>	<b>Kristensen's 4°C</b>	<b>Kristensen's RT</b>
<b>Time</b>	33 days	31 days	33 days	18 days	18 days
<b>Microscopic morphology preservation</b>	Very good	Very good	Very good	Very good	Very good
<b>Antigenicity conservation (IHC)</b>	Very good	Very good	Very good	Very good	Very good

OA causes decreased cartilage thickness and increased cell density, cell size and number of clusters

Since we would like to investigate if anti-DKK1 and anti-FRZB VHHs can induce osteoarthritic-like symptoms, typical symptoms of OA were determined and quantified. This makes it possible to compare the results of the experiment with VHHs to a standard. Human osteochondral plugs were obtained of which two were macroscopically healthy and two were osteoarthritic. The plugs were evaluated for the thickness of the different zones, the cell density, the cell size, the number of clusters and the location of the staining.

As can be seen in figure 17, preserved (macroscopically healthy) and OA samples showed great macroscopic differences. Based on the histological features, the severity of OA was represented by scores from 0-5 assessing structural damages and cellular abnormalities according to the OARSI guidelines. The two preserved samples got an OARSI grade of 1. The surface showed some superficial fibrillations, but there were no cellular abnormalities. In addition, the superficial layer showed a loss in Safranin O staining. The two OA samples are scored OARSI grade 3 and 4. The grade 3 sample showed great loss of Safranin O staining into the lower 2/3 of the cartilage and a great reduction of the cartilage thickness. Lastly, the grade 4 sample showed erosion and hypertrophic cluster formation. In the preserved sample no hypertrophic clusters were observed, while the grade 3 sample showed  $\pm$  20 hypertrophic clusters and the grade 4 sample even >60 hypertrophic clusters.

Furthermore, the thickness of the superficial, middle and deep zones were measured in the preserved sample. The different zones were easily distinguishable by the typical cell arrangement; flat cells in the superficial zone, few round cells in the middle zone and columns of cells in the deep zone. Figure 18A shows that the superficial layer was only a small part of the total thickness. The middle zone comprised most of the cartilage and the deep zone around 40%. Based on these measurements the expected zoning of the OA samples was determined. The OA grade 3 sample consisted of the deep zone and a part of the middle zone. This can also be seen based on the cellular arrangements. The middle zone of this sample had almost lost all Safranin O staining. Some cells still showed some staining in the pericellular matrix as also can be seen in the superficial layer of the preserved sample. The grade 4 sample consisted only of the deep zone based on its thickness. In fact, there was no clear zoning left anymore. The top part of the sample showed highly hypertrophic clusters of cells, while the lower part of the deep zone still showed some column formation of cells.

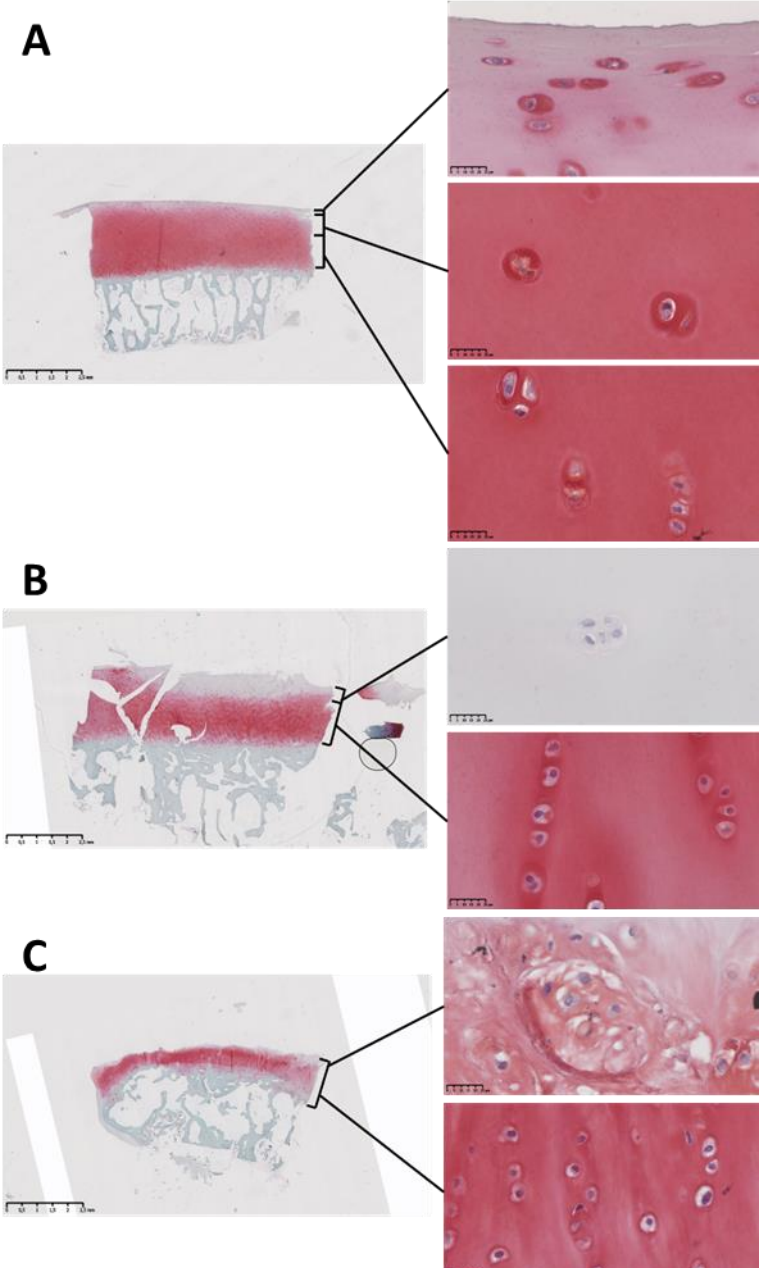


Figure 17: (A) Safranin O staining preserved sample with clear distinction on zones based on the cellular morphology. (B) Grade 3 OA sample with a small part of the middle zone, which lost all Safranin O staining, and a nicely arranged deep zone. (C) Grade 4 OA sample in which almost all structure is lost.

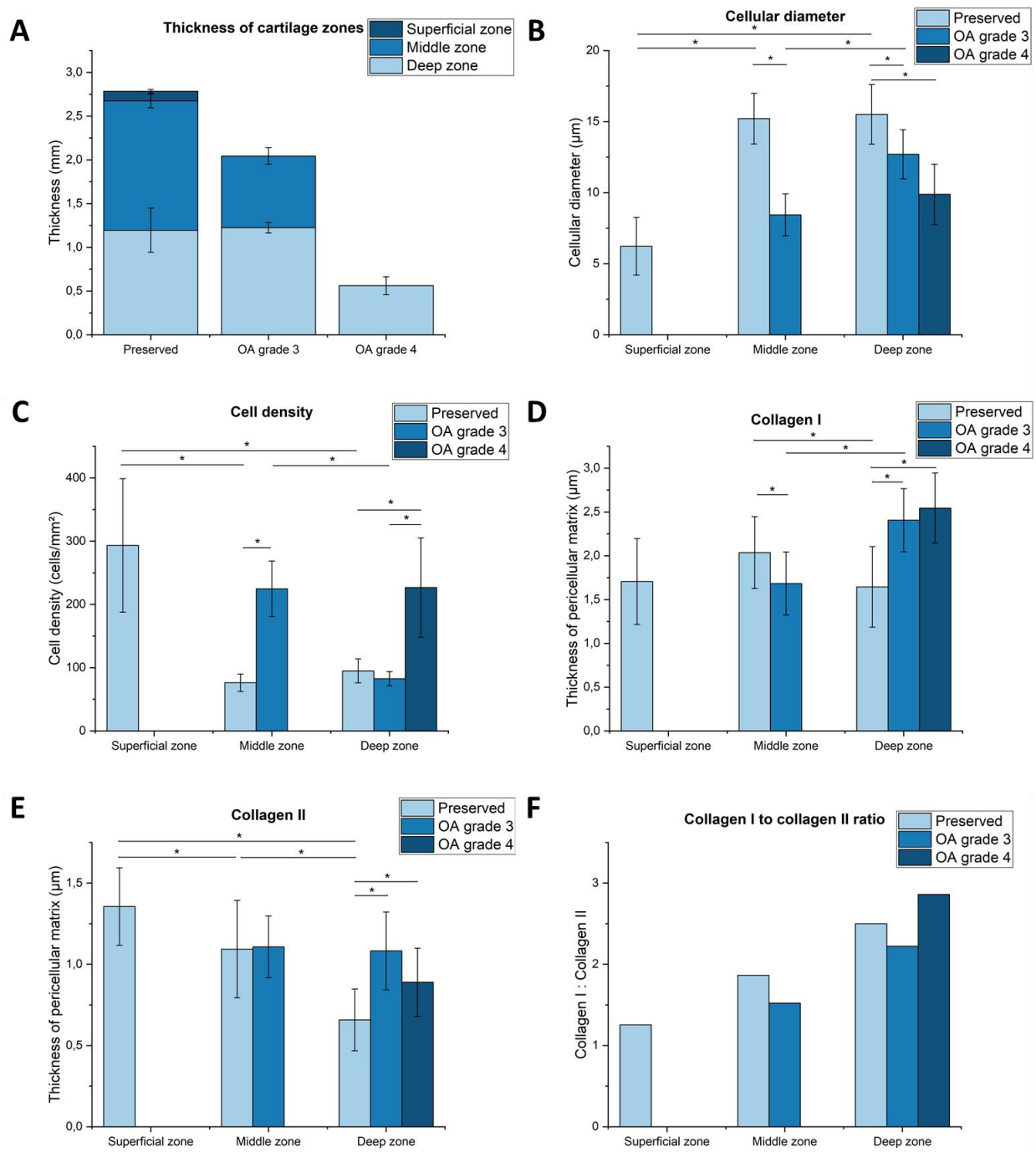


Figure 18: Safranin O and IHC stained images were analysed and lead to the quantification of (A) the thickness of the different zones in the articular cartilage of a preserved sample, OA grade 3 sample and OA grade 4 sample (n=3), (B) the cellular diameter, (C) the cell density, (D) the pericellular matrix thickness of collagen I, (E) the pericellular matrix thickness of collagen II and (F) the ratio of collagen I to collagen II pericellular matrix thickness. For the preserved samples 2 samples 10 points each were measured, for the OA samples 10 different points were measured for graph B-E. The average  $\pm$  SD is visualized. \*P<0.05

The cellular diameter and cell density were also analysed. The cellular diameter increased from the superficial zone to the deep zone, while the cell density decreased from the superficial zone to the deep zone as shown in figure 18B and C. The OA grade 4 sample had the smallest cellular diameter in the deep zone. The OA grade 3 sample had a larger cellular diameter in the deep zone, but still a smaller diameter than the cells in the preserved sample. The diameter of the cells of the OA grade 3 sample in the middle zone had the same diameter as the cells in the deep zone of the OA grade 4 sample. In addition, the cell density of the OA grade 3 sample was higher in the middle compared to the preserved sample. In the deep zone the cell density was similar. The cell density of the OA grade 4 sample, which only has a deep zone, was a lot higher than that of the preserved and OA grade 3 sample in the deep zone.

The samples were also stained for collagen I and collagen II (figure 19). The collagen I staining was mostly located around the cells in the pericellular matrix as can be seen by the dark brown staining around the cells. The thickness of the pericellular matrix of collagen I did not change a lot throughout the zones of the preserved sample (figure 18D). The pericellular matrix was a bit thicker in the middle zone than the superficial and deep zone. The OA samples showed an increased collagen I pericellular matrix in the deep zone compared to the preserved sample. Collagen II was also located in the pericellular matrix. The pericellular matrix was less bright and in general less thick as that of collagen I. The thickness of the collagen II pericellular matrix decreased when getting deeper in the preserved articular cartilage (figure 18E). The OA samples showed a larger collagen II pericellular matrix in the deep zone than the preserved sample. When looking at the ratio of collagen I to collagen II, it can be observed that the ratio increased the deeper you go into the preserved cartilage. The ratio did not change much in the deep zone when comparing the preserved and OA samples (figure 18F).

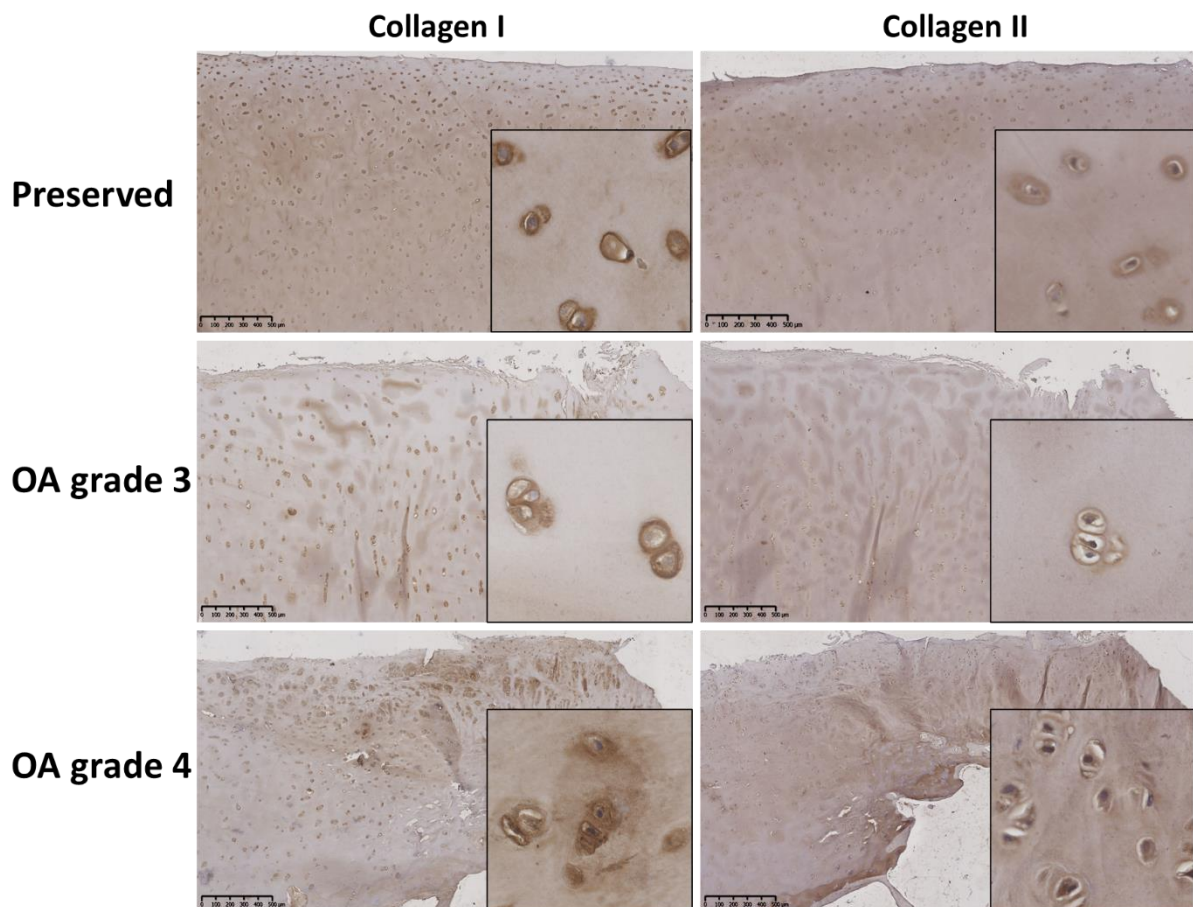


Figure 19: The protein expression of collagen type I and collagen type II was visualized by IHC. (A) Representative pictures are shown. Images were taken using the Nanozoomer.

## DKK1 and FRZB biological activity

### DKK1 and FRZB neutralize WNT3a activity

It is known that DKK1 and FRZB are WNT pathway antagonist. The ability of DKK1 and FRZB to neutralize WNT pathway agonist BIO and WNT3a was determined. The optimal BIO and WNT3a stimulation concentrations were determined at 1  $\mu$ M and 100 ng/ml. Afterwards a concentration range of DKK1 or FRZB was added. It was expected that the addition of DKK1 and FRZB to BIO stimulated cells will show similar activity to only BIO stimulated cells. The addition of DKK1 or FRZB to WNT3a stimulated cells was expected to downregulate the WNT pathway activity to similar levels as the control.

Figure 20A shows that the addition of BIO resulted in an upregulation of the WNT pathway activity of fivefold. The addition of DKK1 and FRZB resulted in an upregulation similar to only BIO stimulation. Figures 20B and C show that the addition of WNT3a resulted in an six-fold upregulation. Once DKK1 was added, the activity decreased in a concentration-dependent manner. The addition of 300 ng/ml (16 nM) resulted in complete neutralization of 100 ng/ml (2.67 nM) WNT3a induced activity. The same was visible for FRZB. The addition of FRZB resulted in a downregulation of the WNT3a induced activity in a concentration-dependent manner. It seems that 100 ng/ml (3.01 nM) was already enough to neutralize WNT3a. When adding only DKK1 or only FRZB, the WNT pathway activity was upregulated.

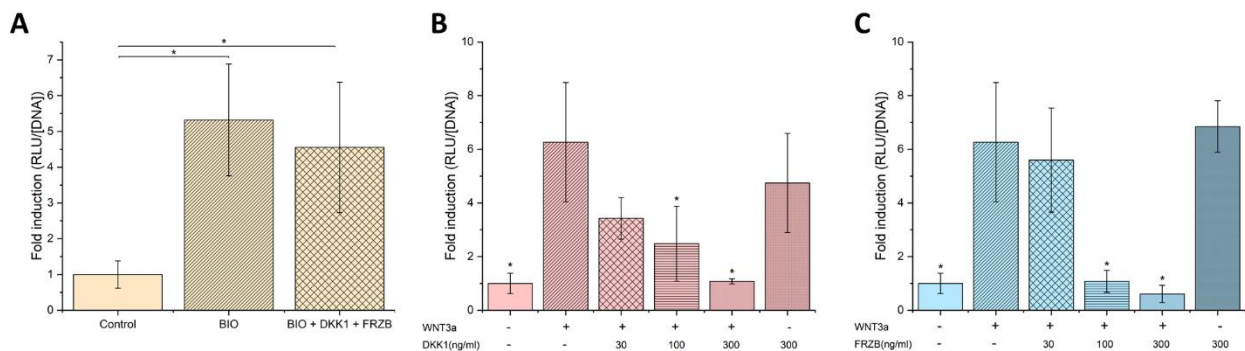


Figure 20: (A) Addition of BIO stimulates WNT pathway activity in C2C12 cells. Co-incubation with DKK1 and FRZB did not show any decrease in activity. (B) Addition of WNT3a stimulates WNT pathway activity. Co-incubation with DKK1, neutralized WNT3a in a concentration-dependent manner. (C) Co-incubation of WNT3a with FRZB, also neutralized WNT3a in a concentration dependent manner. \* $p < 0.05$  versus control.

## Anti-DKK1 and anti-FRZB VHH biological activity and binding characteristics

### Anti-DKK1 and anti-FRZB VHHs do not neutralize DKK1 and FRZB activity

In order to simulate the decreased presence of DKK1 and FRZB in OA, VHHs were developed to competitively bind DKK1 or FRZB. Before using the VHHs in osteochondral plugs, it needs to be investigated if the VHHs can neutralize DKK1 or FRZB activity. A dose-response experiment was performed to determine the optimal VHH concentration for blocking.

In figure 21A, it can be seen that WNT3a induced WNT pathway activity three-fold. Co-incubation with 300 ng/ml DKK1 almost completely neutralized WNT3a activity. The next step was to add a concentration range of anti-DKK1 VHHs. The addition of anti-DKK1 VHHs resulted in a WNT pathway activity similar to the co-incubation of WNT3a with DKK1. In figure 21B, it can be seen that WNT3a induced WNT pathway activity two-fold. Co-incubation with FRZB slightly reversed WNT3a activity. The addition of multiple concentrations of anti-FRZB VHHs, did not block FRZB activity. Both VHHs did not neutralize DKK1 and FRZB.

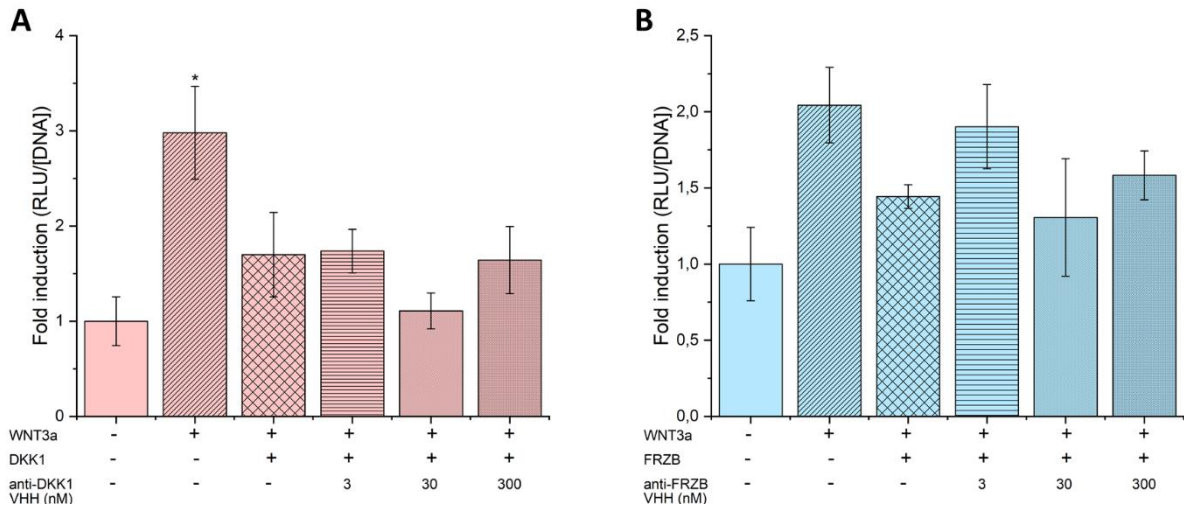


Figure 21: Addition of WNT3a stimulates WNT pathway activity. Co-incubation with DKK1 or FRZB, neutralized WNT3a in a concentration dependent manner. The addition of (A) anti-DKK1 VHHs or (B) anti-FRZB VHHs does not block DKK1 or FRZB activity. \* $p < 0.05$  versus control.

Anti-DKK1 VHH binds strongly to rhDKK1, anti-FRZB VHH binds very weakly to rhFRZB

Since the VHHs did not block DKK1 or FRZB, the binding affinities of the VHHs to recombinant human (rh)DKK1 or rhFRZB were determined to see if there is binding. The binding affinities were determined using an indirect titration ELISA. The binding curves are shown in figure 22. Both VHHs bind to the recombinant protein they are designed to bind to. Anti-FRZB showed really low binding affinity, since it only bound at a high concentration of rhFRZB. The apparent affinity of anti-DKK1 VHH to rhDKK1 was (EC<sub>50</sub>)  $3.4 \times 10^{-10}$  M. The apparent affinity can be determined more accurately using SPRI. Gerben ten Hag has done this and determined it at  $K_D = 9.1 \times 10^{-10}$  M. The apparent affinity of anti-FRZB VHH could not be determined. The smaller the apparent affinity, the stronger the binding to the protein.

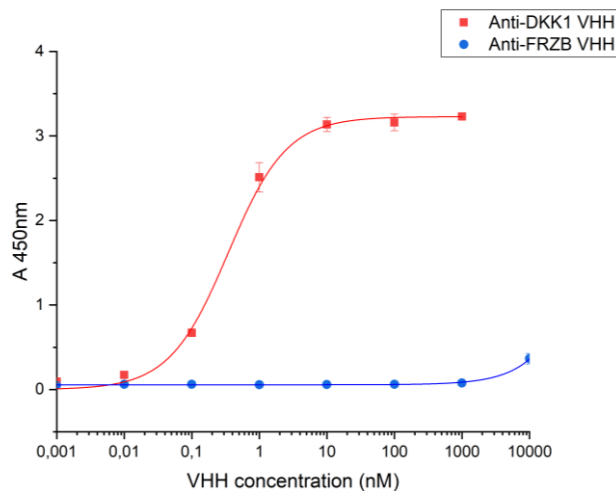


Figure 22: An indirect titration ELISA was performed and resulted in two binding curves.

Anti-DKK1 and anti-FRZB VHHs bind to bCh cell lysate, but not to rhDKK1 or rhFRZB

The binding affinities of the VHHs to the recombinant human proteins were determined. However, because of a lack of available healthy human material, the effect of the VHHs will be determined using bovine osteochondral plugs. Therefore, it needs to be investigated whether the VHHs also bind to bovine DKK1 and bovine FRZB.

A protein-protein comparison was performed using the NCBI BLAST (basic local alignment search tool) analysis tool to compare the amino acid sequence of human DKK1 and bovine DKK1 and human FRZB and bovine FRZB [43]. The amino acid sequences of the proteins were compared to give insight in the probability that human DKK1 and FRZB could bind to their bovine counterparts. Human DKK1 and bovine DKK1 showed 90.7% similarity, while human FRZB and bovine FRZB showed 96.3% similarity. Similarity of the proteins is defined as the extent to which two sequences have the same residues at the same position in an alignment [40]. The similarity is high, but dependent on the binding domain of the proteins. If the proteins bind in the small areas that they are not homologous, they might not bind.

The binding ability of VHHs to the bovine proteins was determined using a dot blot. As a control to check if the secondary antibody binds to the VHHs, anti-DKK1 and anti-FRZB VHHs were blotted. As shown in figure 23, a bright dot was developed for the anti-DKK1 VHH. The dot for anti-FRZB was not that bright, but still visible. The affinity of the rabbit anti-lama secondary antibody was higher for anti-DKK1 than for anti-FRZB VHH.

Secondly, rhDKK1 and rhFRZB were blotted at different concentrations. The VHHs were designed to bind to the human proteins and were therefore expected to bind and show a bright dot. However, as can be seen, no dot was visible. The VHHs did not bind to the rhDKK1 or rhFRZB.

Lastly, bChs lysate was blotted without denaturing or blotted after heating to 90°C in RIPA buffer at different concentrations. The anti-DKK1 VHH showed concentration dependent binding to the unheated cell lysate. The same was true for the heat-denatured cell lysate, however, the dots appeared less bright. For the 10x diluted heat-denatured cell lysate there was no dot visible anymore. In addition, the anti-FRZB VHH also bound concentration dependently to unheated cell lysate. There was no dot visible anymore for the 10x diluted unheated cell lysate. It was almost not visible anymore, but the anti-FRZB VHHs also bind to the undiluted and 2x diluted heated cell lysate. So, the human anti-DKK1 and anti-FRZB VHHs bind to a protein in the bovine cell lysate concentration and denaturation dependently.

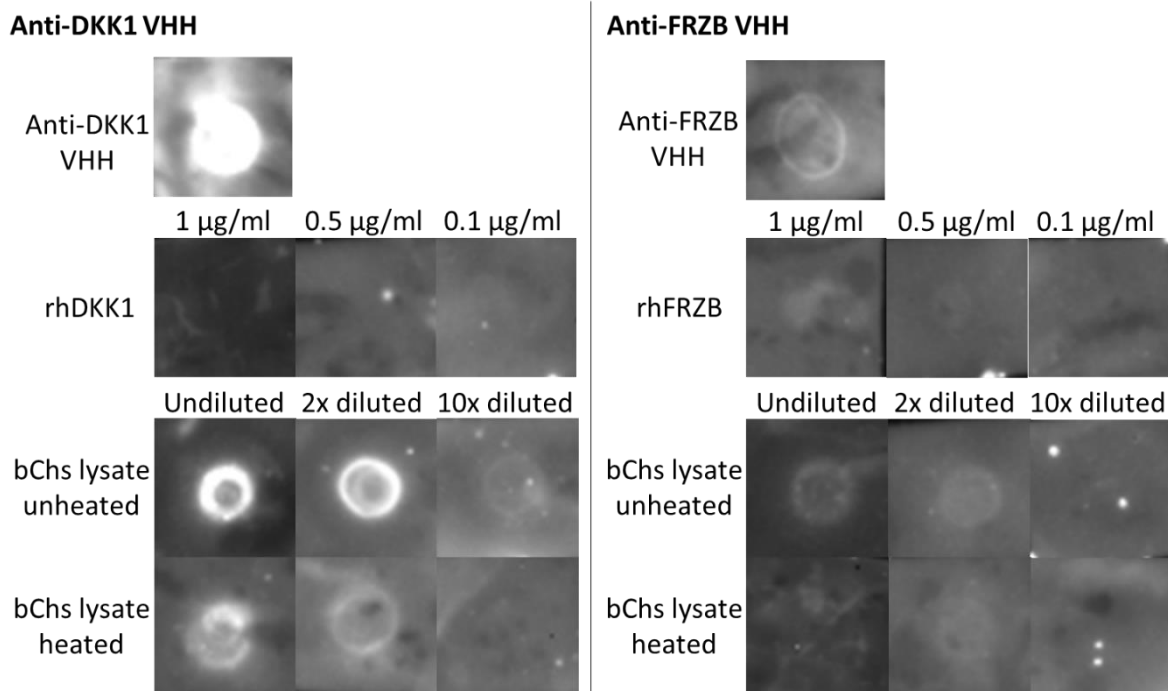


Figure 23: Dot blot to determine anti-DKK1 and anti-FRZB VHH binding ability to bovine DKK1 and FRZB. Binding of the secondary antibody to the VHHs is shown at the top. There is no binding visible to the recombinant human proteins. Binding of the VHHs to the bChs lysate is observed in a concentration and heated/unheated dependent manner. (n=1)

## Discussion

### Experimental set-up characterization

#### Isolated bChs for control experiments

The possibility to utilize isolated bovine chondrocytes from articular cartilage as control cells for future osteochondral plug experiments was investigated by analyzing typical gene expression profiles. *AXIN2* is a direct target of WNT signalling mediated through TCF/LEF factors. WNT pathway agonist WNT3a and BIO should therefore be able to upregulate *AXIN2* expression [73]. As can be seen in figure 11, *AXIN2* gene expression was in fact upregulated upon WNT pathway stimulation.

Furthermore, it was expected that *COL2a1* and *ACAN* would be downregulated upon WNT pathway stimulation [74][75]. Upon BIO stimulation it could be observed that *ACAN* and *COL2a1* gene expression were downregulated as expected. However, WNT3a did not downregulate *ACAN* expression. *ACAN* downregulation upon WNT3a stimulation might only be observable after an extended time of stimulation.

*COL2a1* expression was downregulated after 24h of stimulation, after which an increase in *COL2a1* expression was observed. This increase in collagen II expression after 48h and 72h of stimulation was also visible for BIO stimulation. It has been mentioned by Poole et al. that early-stage collagen II loss is accompanied by an increased synthesis of damaged collagen II [76]. This could be what is observed in figure 11C.

Lastly, *COL10a1* was upregulated upon BIO and WNT3a stimulation. This is in line with literature, which states that the addition of WNT pathway stimulation, upregulates *COL10a1* expression [77]. To conclude, the isolated chondrocyte behaved as expected and similar as hChs to stimulation of the WNT signalling pathway and therefore the bChs can be used as a control for future experiments.

#### Long-term culture of bovine osteochondral plugs

It has been shown by Schwab et al. [64] that osteochondral plugs from pigs can be cultured for 56 days in the *ex vivo* osteochondral culture platform under controlled conditions, while maintaining cartilage tissue content, structure, and mechanical properties. Kleuskens et al. [66] showed that using the same platform, human osteochondral plugs can be cultured stably for at least 28 days. Demonstrating the application of this platform to other species is necessary. Therefore, in this study it is shown that bovine osteochondral plugs can be cultured for 28 days without the loss of staining intensity. This staining intensity is related to the GAG content. Therefore, it was thought that the GAG content remained stable over the culture period as expected. Furthermore, the structure of the osteochondral plugs had remained intact. A smooth surface could be observed. Likewise, the superficial, middle and deep zone could be recognized.

Nevertheless, the chondrocyte viability has not been evaluated in this study. In earlier studies, it has been shown that chondrocyte viability in the core was maintained, but chondrocyte viability in the periphery dropped in some samples. This has especially been observed in the damaged explants since the shear strain is higher in fibrillated explants than in smooth explants during drilling [66]. In further research, close attention has to be paid to cell viability by performing a MTT or TUNEL assay.

In this study, a two-compartment culture platform was used to culture bone and cartilage, each in their own specific medium, where crosstalk is only possible through the bone-cartilage interface, because de Vries-van Melle et al. showed that cartilage-related gene expression decreased in one compartment cultures [61]. Schwab et al. also investigated GAG content in one compartment cultured osteochondral plugs and found that the GAG content was decreased [64].

To strengthen this claim, it was also investigated if osteochondral plug culture in a well plate with only cartilage medium would decrease GAG content indeed. As can be seen in figure 13B, no loss in staining intensity was observed. It can be possible that a difference in loss of staining between two and one compartment culture can only be observed after a longer period of time using the staining intensity as analysis method.

All in all, it was demonstrated that bovine osteochondral plugs with a smooth cartilage layer can be cultured without the loss of structure or GAG content for at least 28 days. It has not been shown that the *ex vivo* osteochondral culture platform has an advantage over simple one compartment culture regarding culture stability up to 28 days. To evaluate the effect of anti-DKK1 and anti-FRZB VHHs on the induction of osteoarthritis, both culturing methods can be used. In case of the one compartment culture, the plugs can be sliced in half to be able to compare within the same plug.

#### The optimal decalcification method

As a result of the anatomical nature of bone, that is, it being highly calcified, the use of an optimal decalcifying strategy is paramount for the appropriate histopathological study of osteochondral plugs. As different experimental conditions need to be tested and compared in further experiments, it is important to choose a golden standard protocol for optimal preservation and processing to diminish differences caused by that process [72]. Therefore, we investigated five different decalcification methods: 12.5% EDTA (Sigma) at 4°C, 12.5% EDTA at RT, 20% EDTA at 4°C, Kristensen's solution at 4°C and Kristensen's solution at RT. They were evaluated on time, microscopic morphological preservation by histochemical staining, and antigenicity preservation by immunohistochemical staining.

In general, all samples maintained good cell morphology and staining intensity. Similar results were obtained in previous studies [78][79][80]. Some of the samples showed a slight decrease in staining intensity underneath the superficial layer. This was, however, visible in plugs of multiple decalcification methods. When looking at the staining intensity throughout the whole cartilage, no differences in staining intensity were observed.

EDTA is in most studies the decalcification agent of choice to perform IHC stainings, because it causes the least damages to epitopes [72]. Kristensen's, however, can damage the epitopes, because of its acidic nature. The buffering capacity of the acid Kristensen's decalcification agent decreases the chance of damaging antigens. EDTA on the other hand does not act like acids, but binds metallic ions, such as calcium and magnesium. EDTA binds to ionized calcium on the outside of the apatite crystal and as this layer becomes depleted more calcium ions reform from within. The crystal becomes progressively smaller [81]. This process does not damage the epitopes making it suitable for IHC evaluation. The IHC staining ability was evaluated in this study and it was observed that both Kristensen's and EDTA decalcification led to specific IHC staining. No significant differences in intensity were observed. Kristensen's did not destroy epitopes.

Both microscopic preservation and antigenicity preservation were really good. However, there was a difference in time it took to decalcify the osteochondral plugs. Kristensen's was almost two times as fast as EDTA decalcification. This is in line with similar studies [6][82][83] and could save a significant amount of time on the total experiment. To conclude, both Kristensen's and EDTA showed good microscopic morphology and antigenicity preservation. No real differences were observed between 4°C and RT or between 12.5% and 20% EDTA. Kristensen's was a lot faster and is therefore the preferred decalcification method for further experiments.

### Healthy and OA articular cartilage characterization

The cartilage thickness, cellular diameter, cell density, collagen I pericellular matrix and collagen II pericellular matrix give a lot of information on the condition and OA stage of cartilage, since these characteristics change with progression of the disease. Figure 18A shows that the thickness of the cartilage decreased significantly in OA. The thickness is related to the OARSI grade of the cartilage. The higher this grade, the smaller the cartilage thickness. In addition, complete cartilage zones got destroyed. In the end no distinct zoning was left anymore as observed in the grade 4 sample.

The thinning of the cartilage is highly dependent on the region of the cartilage [84]. This is also what was observed, since two relatively healthy and two highly thinned samples were obtained from the same joint. Thinning is known to be largest at the weight-bearing cartilage. The OARSI grade and loss of zoning was also related to the thickness of the cartilage [69] as the grade 4 sample was thinner than the grade 3 sample.

Furthermore, as a result of OA, cells undergo dedifferentiation, become apoptotic, become hypertrophic and/or form clusters. Especially in the deep zone of the cartilage clusters are formed [85]. This is also observed in the OA grade 3 and grade 4 sample, which formed large clusters of cells. The grade 4 sample showed significantly more and larger clusters than the grade 3 sample illustrating the increase in hypertrophic cluster formation throughout the progression of OA.

Hypertrophic cluster formation is related to the remodelling of the pericellular matrix. In cartilage, the pericellular matrix is a specialised, thin layer of the ECM that immediately surrounds chondrocytes [86] [87]. A chondrocyte with its pericellular matrix is called a chondron. As can be seen in figure 17, chondrons are arranged differently throughout the cartilage. In OA, it is typically seen that large hypertrophic clusters are formed. This was also observed in the OA grade 4 sample. It was difficult to measure the thickness of the pericellular matrix as it became a connected pericellular matrix of all cells in the clusters. The remodelling of the pericellular matrix is a hallmark of OA and is visualised in figure 24 [88][89].

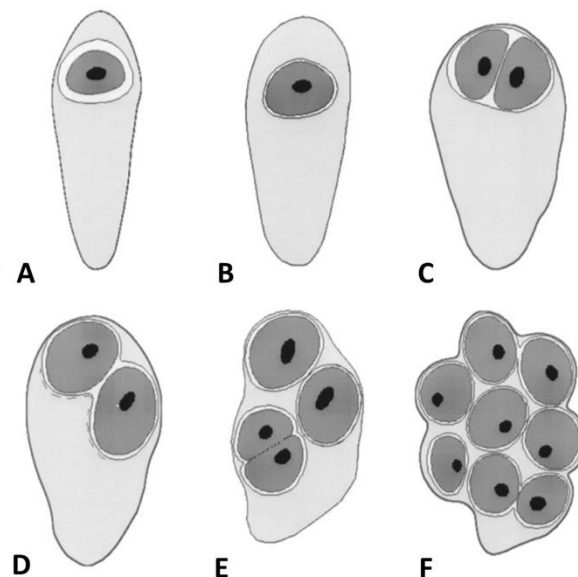


*Figure 24: Schematic overview of the progressive structural changes during chondron remodelling. (A, B) Initially the chondron expands due to a decreased tensile capacity of the fibrillar collagens. (C, D) In the following phase, the decrease of fibrillar collagens continues, the progenitor chondrocyte proliferates and the chondron migrates to the swollen area. (E, F) In the final phase, the chondrocytes completely occupy the swollen microenvironment [89].*

The pericellular matrix made up from collagen I and collagen II was measured from the IHC staining. We observed that the pericellular matrix of collagen II decreased when going deeper into the cartilage. On the other hand, it was discovered that the OA samples showed increased collagen II pericellular matrix thickness in the deep zone. This can be explained based on the mechanical loading on the tissue. In response to dynamic compression, chondrons upregulate the expression of collagen II [88][90][91]. In the preserved sample, the weight is mostly on the superficial zone and decreases throughout the cartilage. Therefore, this decrease in collagen II pericellular matrix thickness can be observed. The OA grade samples had a decreased thickness, therefore, the load bearing function had been taken over by the chondrons in the deeper layers. These chondrons started to produce additional collagen II. Furthermore, chondrons have in general a larger pericellular matrix in OA.

Furthermore, it was noticed that the collagen I pericellular matrix was, in general, larger than the collagen II pericellular matrix. In addition, collagen I pericellular matrix thickness was increased in the deep zone of the OA samples compared to the preserved sample. In the pericellular matrix of healthy chondrocytes, collagen I is not expected to be present, because mainly collagen II, VI and IX are known to be present [92]. However, it has been found recently that collagen I is present in the pericellular matrix of early stage OA chondrocytes due to dedifferentiation [30][93][94]. This could explain the presence of the relatively large collagen I pericellular matrix in the preserved samples. The preserved samples were graded at grade 1, since they showed superficial fibrillations and GAG loss in the superficial layer. Therefore, probably really early stage OA chondrocytes with collagen I expression were found in the preserved samples. Collagen I expression increases during OA progression, which is why an increase in collagen I pericellular matrix thickness was observed in the deep zone of OA samples.

The cell density in the preserved samples was decreased going deeper into the cartilage, but it was constant in the middle and deep zone. This is exactly in line with literature, which also states that the cell density is the highest in the superficial zone and decreases deeper in the cartilage [8]. The cell density increased significantly in the middle zone for the OA grade 3 sample and in the deep zone for the OA grade 4 sample. This can be explained by the fact that OA chondrocytes have a proliferative capacity probably due to the better access to growth factor because of the loosened ECM and the existence of fissures [30]. The increase in cell density can also be seen in the schematic overview of the chondron remodelling in figure 24. The chondron increases in size due to decreased tensile capacity of the fibrillated collagens. Consequently, the chondrocyte proliferates in the increased chondron until it is completely full. On the other hand, it has also been suggested that cell density decreases because cells undergo apoptosis in OA, however, this happens less than thought [30].

Lastly, Onyekwelu et al. claimed that the cell volume increases when going deeper into the cartilage [8]. This is also what we observed (figure 18B) in the preserved sample when measuring the vertical cellular diameter. The superficial zone chondrocytes had a smaller cellular diameter than the middle and deep zone chondrocytes, which had similar cellular diameter. The cells take on a certain shape based on mechanical loading. The compressive forces naturally flatten the cells in the superficial layer, thereby increasing the tension on the cell membrane. The cell volume is decreased to get back to tension levels similar to no compression [95]. The compression is lower in the middle and deep zone. That is why an increase in cellular diameter was observed. Additionally, the cellular diameter of the chondrocytes in the middle zone and deep zone of the OA grade 3 sample and the deep zone of the OA grade 4 sample was smaller compared to the chondrocytes of the preserved sample in the same area. This can be explained by the increase in compressive forces in the middle and deep zone of these samples. Since the zones on top have disappeared, the same forces now act on a deeper layer in the cartilage.

It can be concluded that during OA progression, cartilage thickness decreases. The more severe the OA grade, the more the cartilage is degraded. Due to the loss of cartilage, the mechanical loading changes on the deeper zones of the cartilage, resulting in a decreased cellular diameter and increased collagen II pericellular matrix thickness in the deep zone. The pericellular matrix remodels during OA progression, which results in the presence of collagen I in the pericellular matrix, the increase in cell density and the formation of clusters. This knowledge can be used to analyse bovine osteochondral plugs subjected to VHHs.

### DKK1 and FRZB biological activity

In figure 20, WNT pathway activity of C2C12 cells was shown upon stimulation with several WNT pathway agonists and antagonists. As expected, we observed that BIO and WNT3a are able to stimulate the WNT pathway. Co-incubation of BIO with DKK1 and FRZB did not downregulate WNT pathway activity, while co-incubation of WNT3a with DKK1 or FRZB did result in the downregulation of the WNT pathway. This has to do with the pathway signalling mechanisms of BIO and WNT3a.

As has been explained, WNT3a binds to the WNT receptor Frizzled and is therefore an extracellular signalling molecule [96]. On the other hand, BIO is an intracellular cell signalling molecule and activates the WNT signalling pathway by blocking GSK-3 $\beta$  as shown in figure 25 [17][52]. Whereas WNT3a activates the WNT pathway upstream, BIO does this downstream in the cascade.

DKK1 and FRZB can block WNT3a activity, because DKK1 and FRZB both block WNT pathway signalling via the Frizzled receptor in the cell membrane. DKK1 does this by blocking WNT/ $\beta$ -catenin signalling through binding to the low density lipoprotein receptor related protein (LRP5/6), which prevents all WNT binding to the coreceptor [17][52][97]. FRZB directly binds to extracellular WNT proteins blocking the interaction of the protein with the Frizzled receptor [98][99]. Since BIO stimulates downstream of the blocked Frizzled receptor, WNT pathway activity is still upregulated in the presence of DKK1 and FRZB. All in all, the biological activity of DKK1 and FRZB was determined and in line with literature. DKK1 and FRZB cannot block BIO signalling, but do neutralize WNT3a signalling concentration dependently.

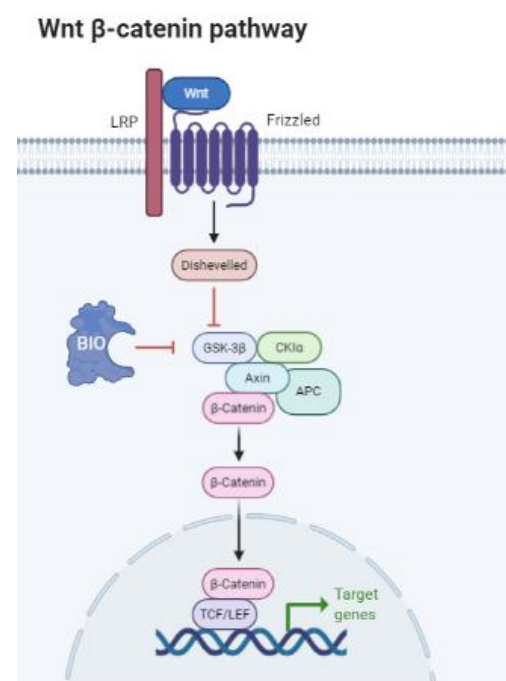


Figure 25: A visualization of the WNT/ $\beta$ -catenin pathway, where intracellular signalling molecule BIO inhibits GSK-3 $\beta$  resulting in an upregulation of the WNT signalling pathway. The binding of DKK1 to LRP 5/6 or the binding of FRZB to all WNT ligands does not change WNT signalling due to BIO. (created in BioRender.com)

### Anti-DKK1 and anti-FRZB VHH biological activity and binding characteristics

Based on the biological activity of DKK1 and FRZB, the biological activities of anti-DKK1 and anti-FRZB VHHs were determined. It was observed that both anti-DKK1 and anti-FRZB did not block WNT3a neutralization of DKK1 or FRZB. However, both Zhong et al. and Rodrigues also determined the biological activity of exactly the same VHHs and found through an alkaline phosphatase assay that the VHHs are able to block FRZB and DKK1 [100][101].

To investigate why the VHHs did not block DKK1 and FRZB activity, binding affinity of the VHHs to rhDKK1 and rhFRZB was redetermined. As can be seen in figure 22, anti-DKK1 VHH showed strong binding to rhDKK1 and anti-FRZB VHH showed weak binding to rhFRZB. The binding affinity of the same VHHs was also determined by Zhong et al. and Rodrigues (figure 26A and B) [52][102]. The shape of the curve for anti-DKK1 H7 and anti-FRZB TSF-1F7 VHHs were the same. For anti-FRZB also no EC50 could be determined. However, when looking at the apparent affinity determined by Rodrigues,  $EC_{50} = 1.1 \times 10^{-7}$  M, and in this thesis,  $EC_{50} = 3.4 \times 10^{-10}$  M, there is a difference of a factor 3. Gerben ten Hag, a bachelor student at DBE in 2018, also performed the same ELISA and found a similar apparent affinity as in this thesis [48]. Therefore, it was decided to continue with a dot blot to determine the binding ability of the VHHs to the bovine proteins to be able to use the VHHs in the experiments with the bovine osteochondral plugs.

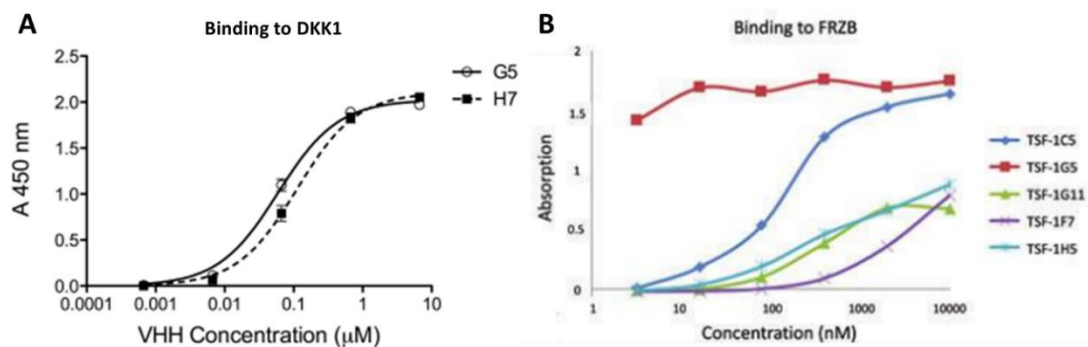


Figure 26: (A) A concentration range of VHH G5 and H7 was incubated in wells coated with DKK1 (60 nM) [17] and (B) a concentration of five different anti-FRZB VHHs as incubated in wells coated with FRZB (60 nM). After several washes, bound VHH were detected with a mouse anti-VHH serum and a Donkey anti-rabbit antibody coupled to a peroxidase. The amount of converted HRP (Absorbance at 450 nm; A 450 nm) is proportional to the amount of bound VHH. Error bars represent standard deviation (N=3). [17]

The VHHs did bind to the bCh cell lysate, but not to the recombinant proteins. In addition, it was observed that there was more binding to the unheated cell lysate than to the heated cell lysate. VHHs are highly resistant to heat. It has been observed that VHHs heated to 90°C, are refolding once added to the antigen [103]. The ability to refold lies between the 0 and 100% and is dependent on intrinsic and extrinsic factors, such as the temperature, time of heating and the VHH itself [104][105]. In the case of the anti-DKK1 and anti-FRZB VHHs, it has been observed that brightness of the dot was lower for the heated VHHs. Probably some of the VHHs have denatured, while also some have refolded and are therefore able to bind the bovine proteins.

So, a couple of unexpected things were observed. First of all, the VHHs did bind to the bCh lysate in the dot blot, but not the recombinant human proteins. This can be caused by the VHHs being aspecific. The VHHs might bind to another protein in the bCh cell lysate instead of to DKK1 and FRZB. On the other hand, binding was observed to rhDKK1 and rhFRZB in the indirect titration ELISA. In addition, the VHHs were generated specifically for DKK1 and FRZB [52]. Therefore, it is more likely that the dot blot procedure needs to be optimized than that the VHHs are aspecific. Nevertheless, to be sure, the specificity of the VHHs need to be determined. The specificity of the VHHs can be determined by a western blot.

Furthermore, the apparent affinity of the VHHs to the recombinant human proteins changed three orders of magnitude between the measurements generated for this thesis/by Gerben ten Hag and by Rodrigues [53]. Different coating densities were used: this thesis 38.8 nM, Gerben ten Hag 19.4 nM and Rodrigues 60nM. It has been found that a different coating density of an antigen can lead to diverse functional affinities [106]. However, Gerben ten Hag and this thesis found exactly the same apparent affinity with a different coating density.

It was discovered that the VHHs used in this thesis, where the same as Rodrigues tested. This means that the VHHs were very old. They have already been used in 2014 or even earlier. The age of the VHHs, storing at  $-30^{\circ}\text{C}$  or repetitive freezing and thawing might have changed VHH folding. VHHs consist of four constant framework regions (FR1-4). These regions are separated by three hypervariable complementary determining loops (CDR1, -2, and -3) [53]. To stabilize the CDR3 loop, it often forms disulfide bonds with the other loops [53]. The formation of these disulfide bonds leads to the formation of an antigen receptor [69][17][17]. The stability of the VHHs is strongly related to specific disulfide bonds between Cysteines. If a disulfide bond is broken or a new one formed, the antigen receptor may change. The new antigen receptor might cause the antigen to bind at a totally different domain and have a different binding affinity. It has been found that, for example, a difference of five amino acids can increase the binding affinity a 1000-fold [64]. All in all, the folding of anti-DKK1 and anti-FRZB VHHs has probably changed due to long-term storage, resulting in different binding characteristics.

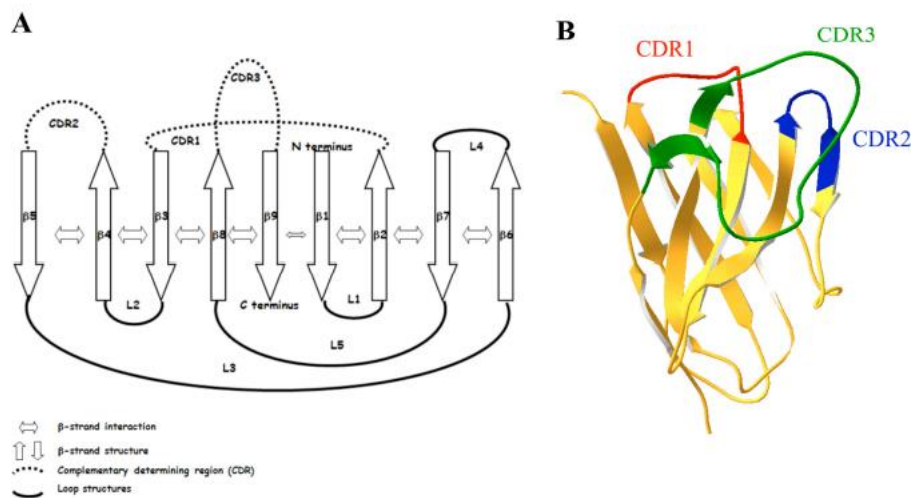


Figure 27: Schematic representation of a VHH and its regions and interactions. (A) A VHH is organized in 9-antiparallel beta-strands connected with loops. The CDR1, -2 and -3 loops form the complementary determining regions. Loops 1, 2, 3 and 5 do not interfere with VHH binding to its antigen. (B) Visualization of a folded VHH [17].

Based on a titration ELISA and dot blot, the binding characteristics of the VHHs were determined. From the dot blot it was concluded that the VHHs do bind to bCh cell lysate. However, the VHHs did not neutralize DKK1 and FRZB activity. Therefore, the VHHs cannot be used for the experiments with the bovine osteochondral plugs. The research question, 'What do anti-DKK1 and anti-FRZB VHH antibodies induce in healthy bovine osteochondral plugs?', cannot be answered at this moment.

## Conclusion

To conclude, this research offers a completely characterized method to analyse anti-DKK1 and anti-FRZB activity in osteochondral plugs. A control cell line has been defined, long-term culture of osteochondral plugs has been established up to 28 days in an *ex vivo* osteochondral culture platform and in a well plate, Kristensen's decalcification solutions has been established as golden standard, and OA has been characterized completely in human osteochondral plugs. Expanding this to the main experiment to investigate if anti-DKK1 and anti-FRZB VHH can induce osteoarthritis, could lead to new insights in the pathogenesis of osteoarthritis. It sets the stage for the development of future therapies to halt the development of osteoarthritis. Unfortunately, current VHHs are not able to block DKK1 and FRZB. Before research can be continued, fresh VHHs need to be evaluated on neutralizing ability, binding affinity and binding ability to bovine DKK1 and FRZB.

## Recommendations

Several things need to be investigated before continuing with anti-DKK1 and anti-FRZB VHH assessment in bovine osteochondral plugs. To know for sure that bovine osteochondral plugs can be cultured for 28 days without degradation of the ECM or loss of cell viability, the cell viability needs to be evaluated using an MTT or TUNEL assay. In addition, freshly ordered VHHs need to be examined on their neutralizing ability, binding affinity and binding ability to bovine DKK1 and FRZB. Luckily the protocols to do so are already defined. In case the fresh VHHs also do not neutralize DKK1 and FRZB activity, the VHH selection process should be repeated.

## References

- [1] D. T. Felson *et al.*, "Osteoarthritis: New insights - Part 1: The disease and its risk factors," in *Annals of Internal Medicine*, 2000, vol. 133, no. 8, pp. 635–646, doi: 10.7326/0003-4819-133-8-200010170-00016.
- [2] R. C. Lawrence *et al.*, "Estimates of the prevalence of arthritis and other rheumatic conditions in the United States. Part II," *Arthritis and Rheumatism*, vol. 58, no. 1, pp. 26–35, Jan. 2008, doi: 10.1002/art.23176.
- [3] Y. Zhang and J. M. Jordan, "Epidemiology of osteoarthritis," *Clinics in Geriatric Medicine*, vol. 26, no. 3. NIH Public Access, pp. 355–369, Aug. 2010, doi: 10.1016/j.cger.2010.03.001.
- [4] E. R. Vina and C. K. Kwok, "Epidemiology of osteoarthritis: Literature update," *Current Opinion in Rheumatology*, vol. 30, no. 2. Lippincott Williams and Wilkins, pp. 160–167, Mar. 01, 2018, doi: 10.1097/BOR.0000000000000479.
- [5] W. Hermann, S. Lambova, and U. Müller-Ladner, "Current Treatment Options for Osteoarthritis," *Current Rheumatology Reviews*, vol. 14, no. 2, pp. 108–116, Jul. 2018, doi: 10.2174/1573397113666170829155149.
- [6] W. Zhang, H. Ouyang, C. R. Dass, and J. Xu, "Current research on pharmacologic and regenerative therapies for osteoarthritis," *Bone Research*, vol. 4, no. 1. Sichuan University, pp. 1–14, Mar. 01, 2016, doi: 10.1038/boneres.2015.40.
- [7] R. E. Rosenberger, A. H. Gomoll, T. Bryant, and T. Minas, "Repair of large chondral defects of the knee with autologous chondrocyte implantation in patients 45 years or older," *American Journal of Sports Medicine*, vol. 36, no. 12, pp. 2336–2344, Dec. 2008, doi: 10.1177/0363546508322888.
- [8] I. Onyekwelu, M. B. Goldring, and C. Hidaka, "Chondrogenesis, joint formation, and articular cartilage regeneration," *Journal of Cellular Biochemistry*, vol. 107, no. 3. J Cell Biochem, pp. 383–392, Jun. 01, 2009, doi: 10.1002/jcb.22149.
- [9] Y. Z. Jiang, S. F. Zhang, Y. Y. Qi, L. L. Wang, and H. W. Ouyang, "Cell transplantation for articular cartilage defects: Principles of past, present, and future practice," *Cell Transplantation*, vol. 20, no. 5. Cell Transplant, pp. 593–607, 2011, doi: 10.3727/096368910X532738.
- [10] W. Zhang, J. Chen, S. Zhang, and H. W. Ouyang, "Inhibitory function of parathyroid hormone-related protein on chondrocyte hypertrophy: the implication for articular cartilage repair," *Arthritis Research and Therapy*, vol. 14, no. 4. Arthritis Res Ther, Aug. 31, 2012, doi: 10.1186/ar4025.
- [11] M. B. Mueller and R. S. Tuan, "Functional characterization of hypertrophy in chondrogenesis of human mesenchymal stem cells," *Arthritis and Rheumatism*, vol. 58, no. 5, pp. 1377–1388, May 2008, doi: 10.1002/art.23370.

- [12] K. M. Hubka, R. L. Dahlin, V. v. Meretoja, F. K. Kasper, and A. G. Mikos, "Enhancing chondrogenic phenotype for cartilage tissue engineering: Monoculture and coculture of articular chondrocytes and mesenchymal stem cells," *Tissue Engineering - Part B: Reviews*, vol. 20, no. 6. Mary Ann Liebert Inc., pp. 641–654, Dec. 01, 2014, doi: 10.1089/ten.teb.2014.0034.
- [13] J. D. Green *et al.*, "Multifaceted signaling regulators of chondrogenesis: Implications in cartilage regeneration and tissue engineering," *Genes and Diseases*, vol. 2, no. 4. Chongqing Medical University, pp. 307–327, Dec. 01, 2015, doi: 10.1016/j.gendis.2015.09.003.
- [14] R. Yasuhara *et al.*, "Roles of B-catenin signaling in phenotypic expression and proliferation of articular cartilage superficial zone cells," *Laboratory Investigation*, vol. 91, no. 12, pp. 1739–1752, Dec. 2011, doi: 10.1038/labinvest.2011.144.
- [15] M. Zhu *et al.*, "Activation of  $\beta$ -catenin signaling in articular chondrocytes leads to osteoarthritis-like phenotype in adult  $\beta$ -catenin conditional activation mice," *Journal of Bone and Mineral Research*, vol. 24, no. 1, pp. 12–21, Jan. 2009, doi: 10.1359/jbmr.080901.
- [16] M. Zhu *et al.*, "Inhibition of  $\beta$ -catenin signaling in articular chondrocytes results in articular cartilage destruction," *Arthritis and Rheumatism*, vol. 58, no. 7, pp. 2053–2064, Jul. 2008, doi: 10.1002/art.23614.
- [17] L. Zhong *et al.*, "Endogenous DKK1 and FRZB Regulate Chondrogenesis and Hypertrophy in Three-Dimensional Cultures of Human Chondrocytes and Human Mesenchymal Stem Cells," *Stem Cells and Development*, vol. 25, no. 23, pp. 1808–1817, Dec. 2016, doi: 10.1089/scd.2016.0222.
- [18] J. C. H. Leijten *et al.*, "Gremlin 1, frizzled-related protein, and dkk-1 are key regulators of human articular cartilage homeostasis," *Arthritis and Rheumatism*, vol. 64, no. 10, pp. 3302–3312, Oct. 2012, doi: 10.1002/art.34535.
- [19] J. C. H. Leijten *et al.*, "GREM1, FRZB and DKK1 mRNA levels correlate with osteoarthritis and are regulated by osteoarthritis-associated factors," *Arthritis Research and Therapy*, vol. 15, no. 5, Sep. 2013, doi: 10.1186/ar4306.
- [20] A. D. Pearle, R. F. Warren, and S. A. Rodeo, "Basic science of articular cartilage and osteoarthritis," *Clinics in Sports Medicine*, vol. 24, no. 1. W.B. Saunders, pp. 1–12, 2005, doi: 10.1016/j.csm.2004.08.007.
- [21] E. K. Moo, N. A. A. Osman, and B. Pinguan-Murphy, "The metabolic dynamics of cartilage explants over a long-term culture period," *Clinics*, vol. 66, no. 8, pp. 1431–1436, 2011, doi: 10.1590/S1807-59322011000800021.
- [22] A. R. Poole, T. Kojima, T. Yasuda, F. Mwale, M. Kobayashi, and S. Lavery, "Composition and structure of articular cartilage: A template for tissue repair," in *Clinical Orthopaedics and Related Research*, 2001, no. 391 SUPPL., doi: 10.1097/00003086-200110001-00004.
- [23] E. B. Hunziker, M. Michel, and D. Studer, "Ultrastructure of adult human articular cartilage matrix after cryotechnical processing," *Microscopy Research and Technique*, vol. 37, no. 4, pp. 271–284, May 1997, doi: 10.1002/(SICI)1097-0029(19970515)37:4<271::AID-JEMT3>3.0.CO;2-O.

- [24] M. B. Goldring and K. B. Marcu, "Cartilage homeostasis in health and rheumatic diseases," *Arthritis Research and Therapy*, vol. 11, no. 3. Arthritis Res Ther, May 19, 2009, doi: 10.1186/ar2592.
- [25] "Articular Cartilage - Basic Science - Orthobullets." <https://www.orthobullets.com/basic-science/9017/articular-cartilage> (accessed Mar. 02, 2021).
- [26] H. Y. Ng, A. A. Lee, and K. X. Shen, "Articular Cartilage: Structure, Composition, Injuries and Repair," 2017. Accessed: Mar. 02, 2021. [Online].
- [27] E. B. Hunziker, "Articular cartilage repair: Basic science and clinical progress. A review of the current status and prospects," *Osteoarthritis and Cartilage*, vol. 10, no. 6, pp. 432–463, 2002, doi: 10.1053/joca.2002.0801.
- [28] S. Hosseinia, L. R. Lindberg, and L. E. Dahlberg, "Cartilage collagen damage in hip osteoarthritis similar to that seen in knee osteoarthritis; a case-control study of relationship between collagen, glycosaminoglycan and cartilage swelling.," *BMC musculoskeletal disorders*, vol. 14, p. 18, Jan. 2013, doi: 10.1186/1471-2474-14-18.
- [29] R. Dreier, "Hypertrophic differentiation of chondrocytes in osteoarthritis: The developmental aspect of degenerative joint disorders," *Arthritis Research and Therapy*, vol. 12, no. 5. Arthritis Res Ther, Sep. 16, 2010, doi: 10.1186/ar3117.
- [30] L. J. Sandell and T. Aigner, "Articular cartilage and changes in arthritis An introduction: Cell biology of osteoarthritis," *Arthritis Research*, vol. 3, no. 2. Arthritis Res, pp. 107–113, 2001, doi: 10.1186/ar148.
- [31] C. M. Thomas, C. J. Fuller, C. E. Whittles, and M. Sharif, "Chondrocyte death by apoptosis is associated with the initiation and severity of articular cartilage degradation.," *International journal of rheumatic diseases*, vol. 14, no. 2, pp. 191–8, May 2011, doi: 10.1111/j.1756-185X.2010.01578.x.
- [32] E. J. Mackie, Y. A. Ahmed, L. Tatarczuch, K. S. Chen, and M. Mirams, "Endochondral ossification: How cartilage is converted into bone in the developing skeleton," *International Journal of Biochemistry and Cell Biology*, vol. 40, no. 1. Int J Biochem Cell Biol, pp. 46–62, 2008, doi: 10.1016/j.biocel.2007.06.009.
- [33] N. Ortega, D. J. Behonick, and Z. Werb, "Matrix remodeling during endochondral ossification," *Trends in Cell Biology*, vol. 14, no. 2. Elsevier Ltd, pp. 86–93, Feb. 01, 2004, doi: 10.1016/j.tcb.2003.12.003.
- [34] Y. Tamamura *et al.*, "Developmental regulation of Wnt/ $\beta$ -catenin signals is required for growth plate assembly, cartilage integrity, and endochondral ossification," *Journal of Biological Chemistry*, vol. 280, no. 19, pp. 19185–19195, May 2005, doi: 10.1074/jbc.M414275200.
- [35] B. Ning *et al.*, "Dual function of  $\beta$ -catenin in articular cartilage growth and degeneration at different stages of postnatal cartilage development," *International Orthopaedics*, vol. 36, no. 3, pp. 655–664, Mar. 2012, doi: 10.1007/s00264-011-1315-6.

- [36] J. R. Hens, K. M. Wilson, P. Dann, X. Chen, M. C. Horowitz, and J. J. Wysolmerski, "TOPGAL mice show that the canonical Wnt signaling pathway is active during bone development and growth and is activated by mechanical loading in vitro," *Journal of Bone and Mineral Research*, vol. 20, no. 7, pp. 1103–1113, Jul. 2005, doi: 10.1359/JBMR.050210.
- [37] F. de Luca *et al.*, "Regulation of growth plate chondrogenesis by bone morphogenetic protein-2," *Endocrinology*, vol. 142, no. 1, pp. 430–436, 2001, doi: 10.1210/endo.142.1.7901.
- [38] A. Vortkamp, K. Lee, B. Lanske, G. v. Segre, H. M. Kronenberg, and C. J. Tabin, "Regulation of rate of cartilage differentiation by Indian Hedgehog and PTH-related protein," *Science*, vol. 273, no. 5275. American Association for the Advancement of Science, pp. 613–622, Aug. 02, 1996, doi: 10.1126/science.273.5275.613.
- [39] J. C. H. Leijten, L. S. Moreira Teixeira, E. B. M. Landman, C. A. van Blitterswijk, and M. Karperien, "Hypoxia Inhibits Hypertrophic Differentiation and Endochondral Ossification in Explanted Tibiae," *PLoS ONE*, vol. 7, no. 11, p. e49896, Nov. 2012, doi: 10.1371/journal.pone.0049896.
- [40] L. Zhong, X. Huang, M. Karperien, and J. N. Post, "The regulatory role of signaling crosstalk in hypertrophy of MSCs and human articular chondrocytes," *International Journal of Molecular Sciences*, vol. 16, no. 8. MDPI AG, pp. 19225–19247, Aug. 14, 2015, doi: 10.3390/ijms160819225.
- [41] M. Blanke, H. D. Carl, P. Klinger, B. Swoboda, F. Hennig, and K. Gelse, "Transplanted chondrocytes inhibit endochondral ossification within cartilage repair tissue," *Calcified Tissue International*, vol. 85, no. 5, pp. 421–433, Nov. 2009, doi: 10.1007/s00223-009-9288-9.
- [42] A. Jikko, Y. Kato, H. Hiranuma, and H. Fuchihata, "Inhibition of chondrocyte terminal differentiation and matrix calcification by soluble factors released by articular chondrocytes," *Calcified Tissue International*, vol. 65, no. 4, pp. 276–279, Mar. 1999, doi: 10.1007/s002239900698.
- [43] F. Yano *et al.*, "The canonical Wnt signaling pathway promotes chondrocyte differentiation in a Sox9-dependent manner," *Biochemical and Biophysical Research Communications*, vol. 333, no. 4, pp. 1300–1308, Aug. 2005, doi: 10.1016/j.bbrc.2005.06.041.
- [44] R. Yasuhara *et al.*, "Roles of B-catenin signaling in phenotypic expression and proliferation of articular cartilage superficial zone cells," *Laboratory Investigation*, vol. 91, no. 12, pp. 1739–1752, Dec. 2011, doi: 10.1038/labinvest.2011.144.
- [45] A. B. Blom *et al.*, "Involvement of the Wnt signaling pathway in experimental and human osteoarthritis: Prominent role of Wnt-induced signaling protein 1," *Arthritis and Rheumatism*, vol. 60, no. 2, pp. 501–512, Feb. 2009, doi: 10.1002/art.24247.
- [46] M. H. Kagey and X. He, "Rationale for targeting the Wnt signalling modulator Dickkopf-1 for oncology," *British Journal of Pharmacology*, vol. 174, no. 24. John Wiley and Sons Inc., pp. 4637–4650, Dec. 01, 2017, doi: 10.1111/bph.13894.
- [47] S. Muyldermans *et al.*, "Camelid immunoglobulins and nanobody technology," *Veterinary Immunology and Immunopathology*, vol. 128, no. 1–3, pp. 178–183, Mar. 2009, doi: 10.1016/j.vetimm.2008.10.299.

- [48] "VHH antibodies as biotherapeutics | Isogenica." <https://www.isogenica.com/vhh-antibodies-as-biotherapeutics/> (accessed Jun. 04, 2020).
- [49] M. M. Harmsen and H. J. de Haard, "Properties, production, and applications of camelid single-domain antibody fragments," *Applied Microbiology and Biotechnology*, vol. 77, no. 1. Springer, pp. 13–22, Nov. 2007, doi: 10.1007/s00253-007-1142-2.
- [50] S. Muyldermans, "Nanobodies: Natural Single-Domain Antibodies," *Annual Review of Biochemistry*, vol. 82, no. 1, pp. 775–797, Jun. 2013, doi: 10.1146/annurev-biochem-063011-092449.
- [51] D. Smolarek, O. Bertrand, and M. Czerwinski, "Variable fragments of heavy chain antibodies (VHHs): A new magic bullet molecule of medicine?," *Postepy Higieny i Medycyny Doswiadczalnej*, vol. 66. Polska Akademia Nauk, pp. 348–358, 2012, doi: 10.5604/17322693.1000334.
- [52] E. D. Rodrigues, *Single Domain Antibodies in Tissue Engineering*. 2014.
- [53] C. S. Bever *et al.*, "VHH antibodies: emerging reagents for the analysis of environmental chemicals," *Analytical and Bioanalytical Chemistry*, vol. 408, no. 22. Springer Verlag, pp. 5985–6002, Sep. 01, 2016, doi: 10.1007/s00216-016-9585-x.
- [54] G. P. Smith and V. A. Petrenko, "Phage display," *Chemical Reviews*, vol. 97, no. 2, pp. 391–410, 1997, doi: 10.1021/cr960065d.
- [55] L. Ledsgaard, M. Kilstrup, A. Karatt-Vellatt, J. McCafferty, and A. H. Laustsen, "Basics of antibody phage display technology," *Toxins*, vol. 10, no. 6. MDPI AG, Jun. 09, 2018, doi: 10.3390/toxins10060236.
- [56] A. C. Chen, J. P. Nagrampa, R. M. Schinagl, L. M. Lottman, and R. L. Sah, "Chondrocyte transplantation to articular cartilage explants in vitro," *Journal of Orthopaedic Research*, vol. 15, no. 6, pp. 791–802, Nov. 1997, doi: 10.1002/jor.1100150602.
- [57] D. W. Hutmacher, "Scaffolds in tissue engineering bone and cartilage," *Biomaterials*, vol. 21, no. 24, pp. 2529–2543, Dec. 2000, doi: 10.1016/S0142-9612(00)00121-6.
- [58] W. Wang, Z. Wang, G. Zhang, C. C. Clark, and C. T. Brighton, "Up-regulation of chondrocyte matrix genes and products by electric fields," in *Clinical Orthopaedics and Related Research*, 2004, no. 427 SUPPL., doi: 10.1097/01.blo.0000143837.53434.5c.
- [59] S. Marino, K. A. Staines, G. Brown, R. A. Howard-Jones, and M. Adamczyk, "Models of ex vivo explant cultures: applications in bone research," *BoneKEy Reports*, vol. 5, Jun. 2016, doi: 10.1038/bonekey.2016.49.
- [60] J. Dumont *et al.*, "Mature full-thickness articular cartilage explants attached to bone are physiologically stable over long-term culture in serum-free media," *Connective Tissue Research*, vol. 40, no. 4, pp. 259–272, 1999, doi: 10.3109/03008209909000704.
- [61] M. L. de Vries-van Melle, E. W. Mandl, N. Kops, W. J. L. M. Koevoet, J. A. N. Verhaar, and G. J. V. M. van Osch, "An Osteochondral Culture Model to Study Mechanisms Involved in Articular Cartilage Repair," *Tissue Engineering Part C: Methods*, vol. 18, no. 1, pp. 45–53, Jan. 2012, doi: 10.1089/ten.tec.2011.0339.

- [62] C. Sanchez, M. A. Deberg, N. Piccardi, P. Msika, J. Y. L. Reginster, and Y. E. Henrotin, "Subchondral bone osteoblasts induce phenotypic changes in human osteoarthritic chondrocytes," *Osteoarthritis and Cartilage*, vol. 13, no. 11, pp. 988–997, Nov. 2005, doi: 10.1016/j.joca.2005.07.012.
- [63] R. Iwai, M. Fujiwara, S. Wakitani, and M. Takagi, "Ex vivo cartilage defect model for the evaluation of cartilage regeneration using mesenchymal stem cells," *Journal of Bioscience and Bioengineering*, vol. 111, no. 3, pp. 357–364, Mar. 2011, doi: 10.1016/j.jbiosc.2010.11.001.
- [64] A. Schwab *et al.*, "Ex vivo culture platform for assessment of cartilage repair treatment strategies," *Altex*, vol. 34, no. 2, pp. 267–277, May 2017, doi: 10.14573/altex.1607111.
- [65] F. Cipriani *et al.*, "Cartilage Regeneration in Preannealed Silk Elastin-Like Co-Recombinamers Injectable Hydrogel Embedded with Mature Chondrocytes in an Ex Vivo Culture Platform," *Biomacromolecules*, vol. 19, no. 11, pp. 4333–4347, Nov. 2018, doi: 10.1021/acs.biomac.8b01211.
- [66] M. W. A. Kleuskens, C. C. Donkelaar, L. M. Kock, R. P. A. Janssen, and K. Ito, "An ex vivo human osteochondral culture model," *Journal of Orthopaedic Research*, p. jor.24789, Jul. 2020, doi: 10.1002/jor.24789.
- [67] K. P. H. Pritzker *et al.*, "Osteoarthritis cartilage histopathology: Grading and staging," *Osteoarthritis and Cartilage*, vol. 14, no. 1, pp. 13–29, Jan. 2006, doi: 10.1016/j.joca.2005.07.014.
- [68] R. G. Pearson, T. Kurien, K. S. S. Shu, and B. E. Scammell, "Histopathology grading systems for characterisation of human knee osteoarthritis - reproducibility, variability, reliability, correlation, and validity," *Osteoarthritis and Cartilage*, vol. 19, no. 3, pp. 324–331, Mar. 2011, doi: 10.1016/j.joca.2010.12.005.
- [69] W. Waldstein, G. Perino, S. L. Gilbert, S. A. Maher, R. Windhager, and F. Boettner, "OARSI osteoarthritis cartilage histopathology assessment system: A biomechanical evaluation in the human knee," *Journal of Orthopaedic Research*, vol. 34, no. 1, pp. 135–140, Jan. 2016, doi: 10.1002/jor.23010.
- [70] L. Zhong, X. Huang, M. Karperien, and J. Post, "Correlation between Gene Expression and Osteoarthritis Progression in Human," *International Journal of Molecular Sciences*, vol. 17, no. 7, p. 1126, Jul. 2016, doi: 10.3390/ijms17071126.
- [71] G. Rolls, "An Introduction to Decalcification." Apr. 22, 2013, Accessed: Oct. 05, 2020. [Online].
- [72] T. Ramírez *et al.*, "Comparison of methods for the histological evaluation of odontocete spiral ganglion cells," *Animals*, vol. 10, no. 4, Apr. 2020, doi: 10.3390/ani10040683.
- [73] E. Jho, T. Zhang, C. Domon, C.-K. Joo, J.-N. Freund, and F. Costantini, "Wnt/ $\beta$ -Catenin/Tcf Signaling Induces the Transcription of Axin2, a Negative Regulator of the Signaling Pathway," *Molecular and Cellular Biology*, vol. 22, no. 4, pp. 1172–1183, Feb. 2002, doi: 10.1128/mcb.22.4.1172-1183.2002.
- [74] R. Yasuhara *et al.*, "Wnt/ $\beta$ -Catenin and retinoic acid receptor signaling pathways interact to regulate chondrocyte function and matrix turnover," *Journal of Biological Chemistry*, vol. 285, no. 1, pp. 317–327, Jan. 2010, doi: 10.1074/jbc.M109.053926.

- [75] T. Yuasa, T. Otani, T. Koike, M. Iwamoto, and M. Enomoto-Iwamoto, "Wnt/b-catenin signaling stimulates matrix catabolic genes and activity in articular chondrocytes: its possible role in joint degeneration," *Laboratory Investigation* |, vol. 88, pp. 264–274, 2008, doi: 10.1038/labinvest.3700747.
- [76] A. R. Poole *et al.*, "Type II collagen degradation and its regulation in articular cartilage in osteoarthritis," doi: 10.1136/ard.61.suppl\_2.ii78.
- [77] A. Held *et al.*, "Targeting  $\beta$ -catenin dependent Wnt signaling via peptidomimetic inhibitors in murine chondrocytes and OA cartilage," *Osteoarthritis and Cartilage*, vol. 26, no. 6, pp. 818–823, Jun. 2018, doi: 10.1016/j.joca.2018.02.908.
- [78] S. Jimson, K. M. K. Masthan, and R. Elumalai, "A Comparative Study in Bone Decalcification Using Different Decalcifying Agents," 2012. Accessed: Feb. 08, 2021. [Online]. Available: [www.ijsr.net](http://www.ijsr.net).
- [79] F. M. Savi, G. I. Brierly, J. Baldwin, C. Theodoropoulos, and M. A. Woodruff, "Comparison of Different Decalcification Methods Using Rat Mandibles as a Model," *Journal of Histochemistry and Cytochemistry*, vol. 65, no. 12, pp. 705–722, Dec. 2017, doi: 10.1369/0022155417733708.
- [80] Y. Shibata, S. Fujita, H. Takahashi, A. Yamaguchi, and T. Koji, "Assessment of decalcifying protocols for detection of specific RNA by non-radioactive in situ hybridization in calcified tissues," *Histochemistry and Cell Biology*, vol. 113, no. 3, pp. 153–159, 2000, doi: 10.1007/s004180050434.
- [81] "Bone | Basicmedical Key." <https://basicmedicalkey.com/bone-6/> (accessed Oct. 05, 2020).
- [82] J. Bao, J. J. Zheng, and D. Wu, "The structural basis of DKK-mediated inhibition of Wnt/LRP signaling," *Science Signaling*, vol. 5, no. 224. Sci Signal, May 15, 2012, doi: 10.1126/scisignal.2003028.
- [83] M. v. Semënov, K. Tamai, B. K. Brott, M. Kühl, S. Sokol, and X. He, "Head inducer dickkopf-1 is a ligand for Wnt coreceptor LRP6," *Current Biology*, vol. 11, no. 12, pp. 951–961, Jun. 2001, doi: 10.1016/S0960-9822(01)00290-1.
- [84] R. J. Buck, W. Wirth, D. Dreher, M. Nevitt, and F. Eckstein, "Frequency and spatial distribution of cartilage thickness change in knee osteoarthritis and its relation to clinical and radiographic covariates - data from the osteoarthritis initiative," *Osteoarthritis and Cartilage*, vol. 21, no. 1, pp. 102–109, Jan. 2013, doi: 10.1016/j.joca.2012.10.010.
- [85] I. Sulzbacher, "Osteoarthritis: Histology and pathogenesis," *Wiener Medizinische Wochenschrift*, vol. 163, no. 9–10, pp. 212–219, May 2013, doi: 10.1007/s10354-012-0168-y.
- [86] L. C. Hughes, C. W. Archer, and I. Ap Gwynn, "The ultrastructure of mouse articular cartilage: Collagen orientation and implications for tissue functionality. A polarised light and scanning electron microscope study and review," *European Cells and Materials*, vol. 9, pp. 68–84, 2005, doi: 10.22203/eCM.v009a09.
- [87] F. Guilak *et al.*, "The pericellular matrix as a transducer of biomechanical and biochemical signals in articular cartilage," in *Annals of the New York Academy of Sciences*, 2006, vol. 1068, no. 1, pp. 498–512, doi: 10.1196/annals.1346.011.
- [88] Z. Zhang, "Chondrons and the Pericellular Matrix of Chondrocytes," *Tissue Engineering - Part B: Reviews*, vol. 21, no. 3, pp. 267–277, Jun. 2015, doi: 10.1089/ten.teb.2014.0286.

- [89] C. A. Poole, "Articular cartilage chondrons : form, function and failure," 1997. Accessed: Feb. 09, 2021. [Online].
- [90] Q. G. Wang, B. Nguyen, C. R. Thomas, Z. Zhang, A. J. el Haj, and N. J. Kuiper, "Molecular profiling of single cells in response to mechanical force: Comparison of chondrocytes, chondrons and encapsulated chondrocytes," *Biomaterials*, vol. 31, no. 7, pp. 1619–1625, Mar. 2010, doi: 10.1016/j.biomaterials.2009.11.021.
- [91] Q. G. Wang *et al.*, "Gene expression profiles of dynamically compressed single chondrocytes and chondrons," *Biochemical and Biophysical Research Communications*, vol. 379, no. 3, pp. 738–742, Feb. 2009, doi: 10.1016/j.bbrc.2008.12.111.
- [92] C. A. Poole, M. H. Flint, and B. W. Beaumont, "Chondrons in cartilage: Ultrastructural analysis of the pericellular microenvironment in adult human articular cartilages," *Journal of Orthopaedic Research*, vol. 5, no. 4, pp. 509–522, 1987, doi: 10.1002/jor.1100050406.
- [93] F. Guilak, R. J. Nims, A. Dicks, C. L. Wu, and I. Meulenbelt, "Osteoarthritis as a disease of the cartilage pericellular matrix," *Matrix Biology*, vol. 71–72. Elsevier B.V., pp. 40–50, Oct. 01, 2018, doi: 10.1016/j.matbio.2018.05.008.
- [94] A. G. Nerlich, I. Wiest, and K. von der Mark, "Immunohistochemical analysis of interstitial collagens in cartilage of different stages of osteoarthrosis," *Virchows Archiv B Cell Pathology Including Molecular Pathology*, vol. 63, no. 1, pp. 249–255, Dec. 1993, doi: 10.1007/BF02899269.
- [95] R. Lewis, C. H. Feetham, and R. Barrett-Jolley, "Cell volume regulation in chondrocytes," *Cellular Physiology and Biochemistry*, vol. 28, no. 6. Cell Physiol Biochem Press, pp. 1111–1122, 2011, doi: 10.1159/000335847.
- [96] Y. Guo *et al.*, "Frzb, a secreted Wnt antagonist, decreases growth and invasiveness of fibrosarcoma cells associated with inhibition of Met signaling," *Cancer Research*, vol. 68, no. 9, pp. 3350–3360, May 2008, doi: 10.1158/0008-5472.CAN-07-3220.
- [97] "Edward Dolk: Stability of llama heavy chain antibody fragments under extreme conditions." <https://dspace.library.uu.nl/bitstream/handle/1874/251/inhoud.htm;jsessionid=59321CAFD2DC3A8939C996394974627F?sequence=16> (accessed Feb. 05, 2021).
- [98] E. R. Goldman, J. L. Liu, D. Zabetakis, and G. P. Anderson, "Enhancing stability of camelid and shark single domain antibodies: An overview," *Frontiers in Immunology*, vol. 8, no. JUL. Frontiers Media S.A., p. 1, Jul. 25, 2017, doi: 10.3389/fimmu.2017.00865.
- [99] G. A. ten Hag, H. B. J. Karperien, J. Prakash, and L. P. Karbaat, "Affecting cellular responses to stimuli using microgels functionalized with VHH," 2018. Accessed: May 25, 2020. [Online].
- [100] Y. Akazawa-Ogawa *et al.*, "Heat-induced irreversible denaturation of the camelid single domain vhh antibody is governed by chemical modifications," *Journal of Biological Chemistry*, vol. 289, no. 22, pp. 15666–15679, May 2014, doi: 10.1074/jbc.M113.534222.
- [101] L. Roth *et al.*, "Isolation of Antigen-Specific VHH Single-Domain Antibodies by Combining Animal Immunization with Yeast Surface Display," in *Methods in Molecular Biology*, vol. 2070, Humana Press Inc., 2020, pp. 173–189.

- [102] C. Ota, H. A. Baarsma, D. E. Wagner, A. Hilgendorff, and M. Königshoff, "Linking bronchopulmonary dysplasia to adult chronic lung diseases: role of WNT signaling," *Molecular and Cellular Pediatrics*, vol. 3, no. 1, Dec. 2016, doi: 10.1186/s40348-016-0062-6.
- [103] P. A. Underwood, "Problems and pitfalls with measurement of antibody affinity using solid phase binding in the ELISA," *Journal of Immunological Methods*, vol. 164, no. 1, pp. 119–130, Aug. 1993, doi: 10.1016/0022-1759(93)90282-C.
- [104] K. A. Henry and C. R. MacKenzie, "Antigen recognition by single-domain antibodies: structural latitudes and constraints," *mAbs*, vol. 10, no. 6. Taylor and Francis Inc., pp. 815–826, Aug. 18, 2018, doi: 10.1080/19420862.2018.1489633.
- [105] D. de Vlieger, M. Ballegeer, I. Rossey, B. Schepens, and X. Saelens, "Single-Domain Antibodies and Their Formatting to Combat Viral Infections," *Antibodies*, vol. 8, no. 1, p. 1, Dec. 2018, doi: 10.3390/antib8010001.
- [106] J. Govaert *et al.*, "Dual beneficial effect of interloop disulfide bond for single domain antibody fragments," *Journal of Biological Chemistry*, vol. 287, no. 3, pp. 1970–1979, Jan. 2012, doi: 10.1074/jbc.M111.242818.
- [107] A. Watanabe, C. Boesch, S. E. Anderson, W. Brehm, and P. Mainil Varlet, "Ability of dGEMRIC and T2 mapping to evaluate cartilage repair after microfracture: a goat study," *Osteoarthritis and Cartilage*, vol. 17, no. 10, pp. 1341–1349, Oct. 2009, doi: 10.1016/j.joca.2009.03.022.

## Supplementary information

### Supplement 1: Primer sequences

Table 2: Primer sequences

Gene name	Primer Sequence	Annealing temperature (°C)
<i>GAPDH</i>	F: 5' GCCATCACTGCCACCCAGAA 3'	60°C
	R: 5' GCGGCAGGTCAGATCCACAA 3'	60°C
<i>AXIN2</i>	F: 5' GAACCTGAAGGATGCCAAAA 3'	60°C
	R: 5' GGTTTCAGCTGCTTGAGAC 3'	60°C
<i>ACAN</i>	F: 5' GACCAGAAGCTGTGCGAGGA 3'	60°C
	R: 5' GCCAGATCATCACCACACAG 3'	60°C
<i>COL2a1</i>	F: 5' ATCAACGGTGGCTTCCACT 3'	60°C
	R: 5' TTCGTGCAGCCATCCTTC 3'	60°C
<i>COL10a1</i>	F: 5' GAATGCCTGTGTCTGCTT 3'	60°C
	R: 5' CGTGTATGTGGTAAGAGAAGT 3'	60°C

### Supplement 2: Long term culture ability Alcian Blue and H&E staining

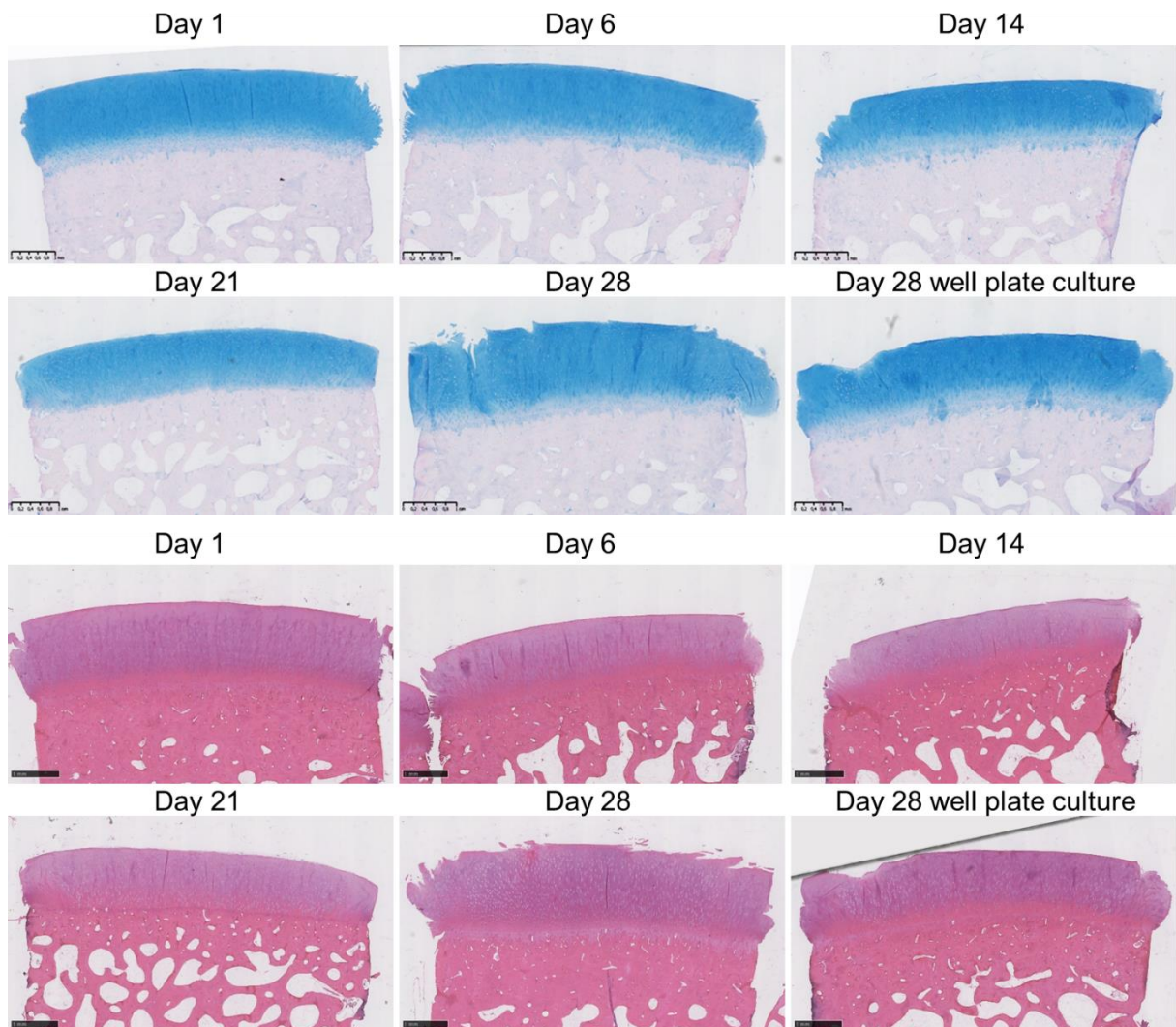


Figure 28: Representative osteochondral plug sections stained with Alcian Blue (Top) and H&E (Bottom). The osteochondral plugs are cultured for 1, 6, 14, 21 and 28 days before they are fixed, decalcified and processed (n=2).

Supplement 3: Decalcification method analysis Alcian Blue and H&E staining

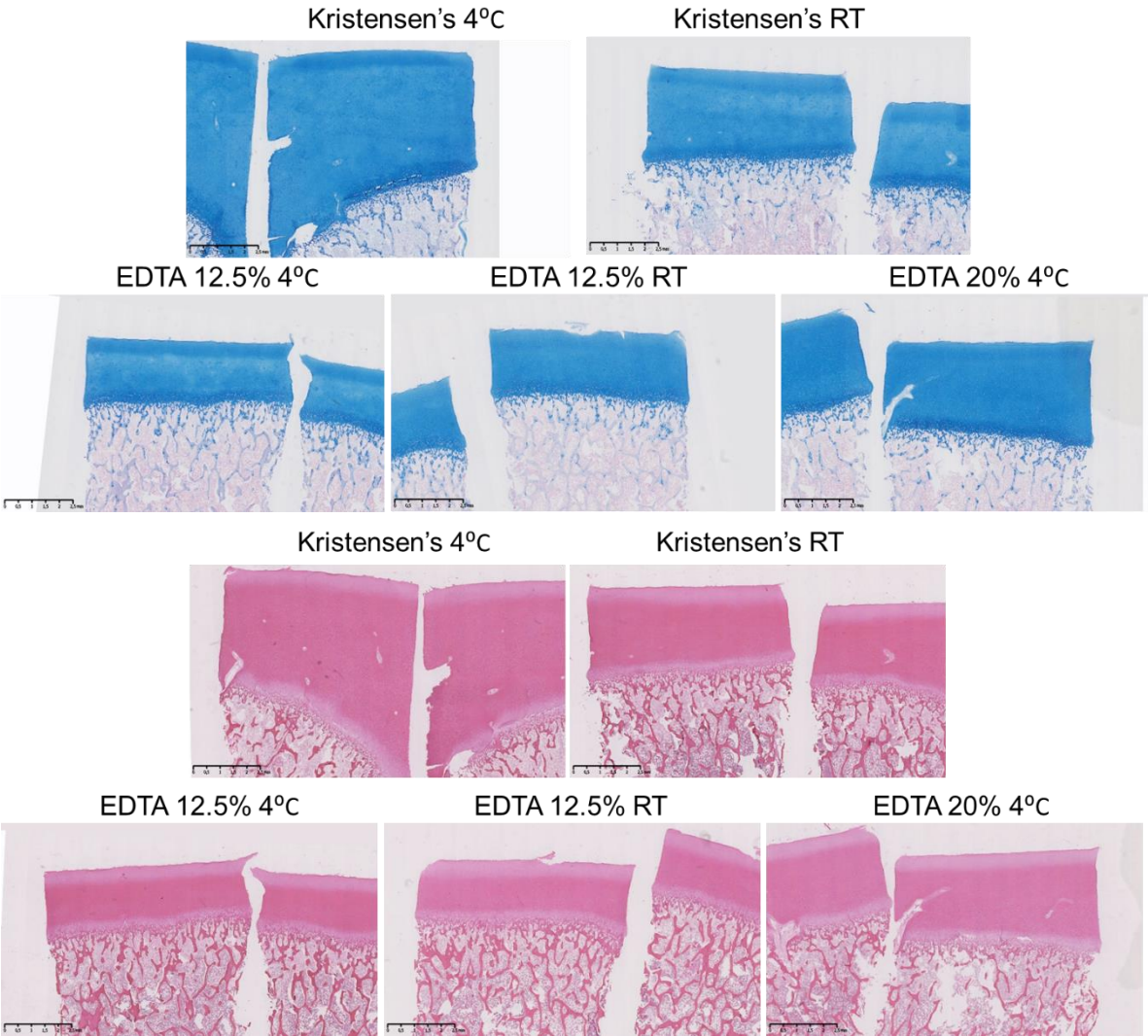


Figure 29: Representative osteochondral plug sections stained with Alcian Blue (Top) and H&E (bottom). The osteochondral plugs are cultured for 5 days before they are fixed, decalcified and processed. For the decalcification five different methods were used: Kristensen's solution at 4°C, Kristensen's solution at RT, 12.5% EDTA at 4°C, 12.5% EDTA at RT and 20% EDTA at 4°C (n=2).

